

วัสดุเชิงประกอบแบบเรียมสตรอนเทียมไททานตกับพอลิอิมิดที่มีค่าคงที่ได้อิเล็กทรอนิกส์สูง

นายชวลิต น้อยภารา

วิทยานิพนธ์นี้เป็นส่วนหนึ่งของการศึกษาตามหลักสูตรปริญญาวิศวกรรมมหาบัณฑิต

สาขาวิชาวิศวกรรมเคมี ภาควิชาวิศวกรรมเคมี

คณะวิศวกรรมศาสตร์ จุฬาลงกรณ์มหาวิทยาลัย

ปีการศึกษา 2554

ลิขสิทธิ์ของจุฬาลงกรณ์มหาวิทยาลัย

บทคัดย่อและแฟ้มข้อมูลฉบับเต็มของวิทยานิพนธ์ตั้งแต่ปีการศึกษา 2554 ที่ให้บริการในคลังปัญญาจุฬาฯ (CUIR)

เป็นแฟ้มข้อมูลของนิสิตเจ้าของวิทยานิพนธ์ที่ส่งผ่านทางบัณฑิตวิทยาลัย

The abstract and full text of theses from the academic year 2011 in Chulalongkorn University Intellectual Repository (CUIR)

are the thesis authors' files submitted through the Graduate School.



HIGH DIELECTRIC CONSTANT OF BARIUM STRONTIUM  
TITANATE/POLYIMIDE COMPOSITES

Mr. Chawalit Noipara

A Thesis Submitted in Partial Fulfillment of the Requirements  
for the Degree of Master of Engineering Program in Chemical Engineering

Department of Chemical Engineering

Faculty of Engineering

Chulalongkorn University

Academic Year 2011

Copyright of Chulalongkorn University



ชวลิต น้อยภารา : วัสดุเชิงประกอบแบบเรียมสตรอนเทียมไททานेटกับพอลิอิมิด์ที่มีค่าคงที่ไดอิเล็กทริกสูง. (HIGH DIELECTRIC CONSTANT OF BARIUM STRONTIUM TITANATE/POLYIMIDE COMPOSITE) อ. ที่ปริกษาวิทยานิพนธ์หลัก: รศ. ดร. ม.ล. ศุภกนก ทองใหญ่, 84 หน้า.

งานวิจัยนี้ศึกษาการเพิ่มค่าคงที่ไดอิเล็กทริกของวัสดุเชิงประกอบด้วยแบบเรียมสตรอนเทียมไททานेटและพอลิอิมิด์ แบบเรียมสตรอนเทียมไททานेट ถูกเตรียมขึ้นด้วยกระบวนการโซลเจล ซึ่งใช้แบบเรียมไฮดรอกไซด์ออกตะไฮเดรต สตรอนเทียมไนเตรตและไททานเนียมไอโซโพรพอกไซด์ เป็นสารตั้งต้น พอลิอิมิด์ถูกเตรียมขึ้นด้วยวิธีการเกิดพอลิเมอร์แบบสองขั้นตอน ซึ่งมี 4,4'-ODA และ PMDA เป็นสารตั้งต้น ผลของขนาดและปริมาณของตัวเติมต่อสมบัติเชิงความร้อนและเชิงไฟฟ้าของวัสดุเชิงประกอบได้แก่ ค่าคงที่ไดอิเล็กทริก ค่าการสูญเสียไดอิเล็กทริกและค่าเสถียรภาพเชิงความร้อนได้ถูกวิเคราะห์ ค่าคงที่ไดอิเล็กทริกของวัสดุเชิงประกอบจะเพิ่มสูงขึ้นตามปริมาณอนุภาคของแบบเรียมสตรอนเทียมไททานेटที่เพิ่มขึ้นและลดลงเมื่อความถี่ของแหล่งกำเนิดเพิ่มขึ้น ผลของการปรับปรุงสภาพผิวอนุภาคของแบบเรียมสตรอนเทียมด้วยสารควบคู่ไฮเลนทั้งสามชนิดต่อสมบัติทางไฟฟ้าของวัสดุเชิงประกอบถูกเปรียบเทียบกับอนุภาคของแบบเรียมสตรอนเทียมไททานेटที่ไม่ได้ถูกปรับปรุงสภาพผิว ซึ่งวัสดุเชิงประกอบที่ปรับปรุงสภาพผิวด้วยสารควบคู่ไฮเลนแสดงค่าคงที่ไดอิเล็กทริกที่ต่ำกว่าวัสดุเชิงประกอบที่ไม่ได้ปรับปรุงสภาพผิวด้วยสารควบคู่ไฮเลน ผลของการไฮบริกขนาดของอนุภาคระหว่างแบบเรียมสตรอนเทียมไททานेटและสตรอนเทียมไททานेट เผยให้เห็นถึงอัตราส่วนโดยน้ำหนักที่เหมาะสมที่สุดสำหรับค่าคงที่ไดอิเล็กทริกสูงสุดเท่ากับ 9:1

ภาควิชา.....วิศวกรรมเคมี..... ลายมือชื่อนิสิต.....  
 สาขาวิชา.....วิศวกรรมเคมี..... ลายมือชื่อ อ.ที่ปริกษาวิทยานิพนธ์หลัก.....  
 ปีการศึกษา...2554.....

## 5370417221: MAJOR CHEMICAL ENGINEERING

KEYWORDS: POLYIMIDE / BARIUM STRONTIUM TITANATE / SURFACE  
MODIFICATION/ EMBEDDED CAPACITOR

CHAWALIT NOIPARA: HIGH DIELECTRIC CONSTANT OF BARIUM  
STRONTIUM TITANATE/POLYIMIDE COMPOSITES. ADVISOR:  
ASSOC.PROF.ML.SUPAKANOK THONGYAI, Ph.D.,  
84 pp.

This research aim is to investigate the dielectric constant of barium strontium titanate( $\text{BaSrTiO}_3$ )/polyimide composite. The  $\text{BaSrTiO}_3$  particles were prepared from barium hydroxide octahydrate, strontium nitrate and titanium (IV) isopropoxide by sol-gel method. The polyimide was prepared by two-step polymerization method, with PMDA and 4'4-ODA as primary materials. The effects of content and size of filler on thermal and electrical properties of  $\text{BaSrTiO}_3$ /polyimide composite including dielectric constant, dielectric loss and thermal stability were investigated. The dielectric constant and dielectric loss of composites exhibited higher values with increasing the  $\text{BaSrTiO}_3$  particles loading and decreased with the frequency of generator increased. The effect of surface modification by three types of silane coupling agents on the dielectric properties of  $\text{BaSrTiO}_3$ / polyimide composite was compared with unmodified composite. The result indicated that the silane coupling agents treated ceramic filler/polyimide composite exhibited lower the dielectric constant and dielectric loss than the unmodified surface composite. The effect of hybrid size of different particles type between  $\text{BaSrTiO}_3$  and  $\text{SrTiO}_3$  were evidenced that the suitable weight ratio between  $\text{BaSrTiO}_3$  and  $\text{SrTiO}_3$  about 9:1 to give the maximum dielectric constant and dielectric loss of composite.

Department : Chemical Engineering .. Student's Signature .....

Field of Study : Chemical Engineering .. Advisor's Signature .....

Academic Year : 2011 .....

## ACKNOWLEDGEMENTS

I would like to express my sincerest gratitude and deep appreciation to my advisor, Associate Professor ML. Supakanok Thongyai, Ph.D. for his kindness, invaluable supervision, invaluable guidance, advices and encouragement throughout the course of his research. I am grateful to Assistant Professor Anongnat Somwangthanaroj, Ph.D., Associate Professor Bunjerd Jongsomjit Ph.D, Assistant Professor Soorathep Kheawhom Ph.D. and Assistant Professor Sirirat Wacharawichanant, D.Eng. for serving as chairman and thesis committees, respectively, whose comments were constructively and especially helpful.

Sincere thanks are made to Mektec Manufacturing Corporation (Thailand) Ltd. for supporting the materials for synthesis polyimide and the characterize equipment, the financial support from the graduate school at Chulalongkorn University, and Department of Chemical Engineering, Faculty of Engineering Chulalongkorn University.

Sincere thanks to all my friends and all members of the Center of Excellent on Catalysis & Catalytic Reaction Engineering (Petrochemical Engineering Research Laboratory), Department of Chemical Engineering, Chulalongkorn University for their assistance and friendly encouragement.

Finally, I would like to dedicate this thesis to my parents and my families, who generous supported and encouraged me through the year spent on this study.

# CONTENTS

	<b>Page</b>
<b>ABSTRACT IN THAI</b> .....	iv
<b>ABSTRACT IN ENGLISH</b> .....	v
<b>ACKNOWLEDGEMENTS</b> .....	vi
<b>CONTENTS</b> .....	vii
<b>LIST OF TABLES</b> .....	x
<b>LIST OF FIGURES</b> .....	xi
<b>CHAPTER I INTRODUCTION</b> .....	1
1.1 The Objective of This Thesis .....	3
1.2 The Scope of This Thesis .....	3
1.3 The Benefits of the Thesis .....	3
<b>CHAPTER II THEORY</b> .....	4
2.1 Polyimide .....	4
2.2 Polyimide synthesis .....	5
2.2.1 One-Step Method .....	5
2.2.2 Two-Step Method .....	7
2.3 Barium strontium titanate .....	9
2.4 Strontium titanate .....	13
2.5 Silane coupling agent .....	14
2.6 The capacitor .....	17
<b>CHAPTER III LITERATURE REVIEWS</b> .....	18
<b>CHAPTER IV EXPERIMENT</b> .....	27
4.1 Materials and Chemicals .....	27
4.2 Equipments .....	28
4.2.1 Barium strontium titanate synthesis part .....	28
4.2.2 Surface modification of barium strontium titanate particle part .....	29
4.2.3 Preparation of polyimide/ barium strontium titanate composite part .....	30
4.3 Barium strontium titanate synthesis .....	31

4.4 Surface modification of barium strontium titanate particles.....	32
4.5 Preparation of polyimide/ barium strontium titanate composites .....	33
4.5.1 Preparation of poly(amic acid).....	33
4.5.2 Preparation of polyimide/ barium strontium titanate composite .....	33
4.5.3 Preparation of polyimide/ barium strontium titanate embedded Capacitor .....	33
4.6 Characterization Instruments .....	34
4.6.1 Infrared Spectroscopy (FTIR).....	34
4.6.2 Scanning electron microscope (SEM) .....	35
4.6.3 Thermogravimetric Analysis (TGA).....	35
4.6.4 X-ray diffraction (XRD) .....	36
4.6.5 LCR meter.....	36
4.6.6 Transmission electron microscopy (TEM) .....	36
<b>CHAPTER V RESULTS AND DISCUSSION.....</b>	<b>37</b>
5.1 Barium strontium titanate synthesis.....	37
5.1.1 Particle size of barium strontium titanate .....	38
5.2 Surface modification of barium strontium titanate particles on composites.....	40
5.2.1 Characterization of silane treated BaSrTiO <sub>3</sub> particles .....	41
5.2.1.1 Functional groups of silane treated BaSrTiO <sub>3</sub> particles.....	41
5.2.1.2 Morphology of untreated and silane treated BaSrTiO <sub>3</sub> particles .....	45
5.2.2 Characterization of silane treated BaSrTiO <sub>3</sub> /polyimide Composite .....	47
5.2.2.1 Functional groups of silane treated BaSrTiO <sub>3</sub> /polyimide composite.....	47
5.2.2.2 Morphology of untreated and silane treated BaSrTiO <sub>3</sub> /polyimide composite.....	51
5.2.2.3 Thermal properties of BaSrTiO <sub>3</sub> /polyimide Composite .....	55
5.2.2.4 Electrical properties of BaSrTiO <sub>3</sub> /polyimide Composite .....	57
5.3 Hybridization of the SrTiO <sub>3</sub> /BaTiO <sub>3</sub> /polyimide composite.....	62



	<b>Page</b>
5.3.1 Morphology of the SrTiO <sub>3</sub> /BaSrTiO <sub>3</sub> /polyimide hybrid composite.....	63
5.3.2 Electrical properties of the SrTiO <sub>3</sub> /BaSrTiO <sub>3</sub> /polyimide hybrid composite.....	65
<b>CHAPTER VI CONCLUSIONS AND RECOMMENDATIONS.....</b>	<b>67</b>
6.1 Conclusions.....	67
6.2 Recommendations.....	68
<b>REFERENCES.....</b>	<b>69</b>
<b>APPENDICES.....</b>	<b>74</b>
<b>APPENDIX A FOURIER TRANSFORM INFRARED SPECTROSCOPY     (FHIR)CHARACTERIZATION .....</b>	<b>75</b>
<b>APPENDIX B EMBEDDED CAPACITOR CHARACTERIZATION.....</b>	<b>80</b>
<b>APPENDIX C THE SIZE DISTRIBUTION OF BST AND     SrTiO<sub>3</sub> PARTICLES.....</b>	<b>82</b>
<b>VITA.....</b>	<b>84</b>

## LIST OF TABLES

	<b>Page</b>
Table 2.1	Properties of general polyimide.....5
Table 2.2	Typical phenolic solvents.....6
Table 2.3	Polyimide monomers.....8
Table 2.4	The ferroelectric and paraelectric properties of perovskite materials ...10
Table 2.5	Typical properties of strontium titanate .....14
Table 5.1	Type and structure of silane coupling agents .....41
Table 5.2	Thermal stabilities of pure PI and BaSrTiO <sub>3</sub> /PI composite .....56

## LIST OF FIGURES

		<b>Page</b>
Figure 2.1	A structure of imide .....	4
Figure 2.2	Aromatic Polyimide Repeat Unit.....	4
Figure 2.3	Two-step method polymerization polyimide synthesis .....	7
Figure 2.4	Perovskite structure of barium strontium titanate .....	9
Figure 2.5	Ferroelectric and paraelectric phases of BST .....	11
Figure 2.6	Basic flow charts for sol-gel process.....	12
Figure 2.7	General structure of strontium titanate.....	14
Figure 2.8	Reaction of silane coupling agents.....	15
Figure 2.9	General structure of silane coupling agents .....	16
Figure 2.10	The mechanisms of silane coupling agent.....	16
Figure 2.11	The structure of capacitor .....	17
Figure 2.12	The capacitor is applied the currents in system .....	17
Figure 3.1	Flow sheet explains the fabrication of ceramic-polymer nanocomposites.....	19
Figure 3.2	Dependence of dielectric constant and electrical conductivity of the PI/LTNO composite films on the volume fraction of LTNO at different frequencies (at 30°C) .....	20
Figure 3.3	Dielectric constant and loss tangent as a function of loading volume of BaTiO <sub>3</sub> particles treated by INAAT and APTS coupling agents and frequency dependence for dielectric constant and dielectric loss of the polyimide/INAAT-treated BaTiO <sub>3</sub> composite .....	21
Figure 3.4	Relative permittivities and loss tangents of the BSTc-COCcomposites and the BSTn-COC composites at 1GHz as a function of BST loading.....	22
Figure 3.5	SEM image of fractured cross surface of the BaTiO <sub>3</sub> -PES composites withBaTiO <sub>3</sub> volume fractions 30% and 50%.....	24
Figure 3.6	Schematic of PI and PI/Al O composite film preparation and reactions involved in the process .....	25

	<b>Page</b>
Figure 3.7	Dielectric constant changes with BaTiO <sub>3</sub> powder load.....26
Figure 4.1	Structures of three types of coupling agents .....28
Figure 4.2	Centrifuge machine .....28
Figure 4.3	Carbolite furnace.....29
Figure 4.4	Ultrasonic .....30
Figure 4.5	Glove box.....30
Figure 4.6	Vacuum oven .....31
Figure 4.7	Embedded capacitor of composite .....34
Figure 4.8	Fourier transform infrared spectroscopy (FTIR) Equipment..... 34
Figure 4.9	Scanning electron microscopy (SEM).....35
Figure 4.10	Thermogravimetric analysis (TGA) equipment..... 31
Figure 4.11	LCR meter ..... 36
Figure 5.1	The XRD patterns of barium strontium titanate .....38
Figure 5.2	SEM micrographs of barium strontium titanate particles at various magnification of SEM equipment.....39
Figure 5.3	TEM micrographs of barium strontium titanate particles.....39
Figure 5.4	The mechanism reaction of silane coupling agents on BaSrTiO <sub>3</sub> surface.....42
Figure 5.5	FT-IR spectra of BaSrTiO <sub>3</sub> particles.....43
Figure 5.6	FT-IR spectra of silane treated BaSrTiO <sub>3</sub> particles.....44
Figure 5.7	Morphology of BaSrTiO <sub>3</sub> particles at ×10k of magnification of SEM equipment.....45
Figure 5.8	Morphology of BaSrTiO <sub>3</sub> particles at ×20k of magnification of SEM equipment.....46
Figure 5.9	FT-IR spectra of pure polyimide .....47
Figure 5.10	FT-IR spectra of pure PI, untreated BaSrTiO <sub>3</sub> /PI composite and Untreated BaSrTiO <sub>3</sub> particles .....48
Figure 5.11	FT-IR spectra of pure PI, APTS silane treated BaSrTiO <sub>3</sub> /PI composite and APTS silane treated BaSrTiO <sub>3</sub> particles .....48
Figure 5.12	FT-IR spectra of pure PI, AEPTS silane treated BaSrTiO <sub>3</sub> /PI composite and AEPTS silane treated BaSrTiO <sub>3</sub> particles .....49

	<b>Page</b>
Figure 5.13 FT-IR spectra of pure PI, AEEPTS silane treated BaSrTiO <sub>3</sub> /PI composite and AEEPTS silane treated BaSrTiO <sub>3</sub> particles.....	49
Figure 5.14 Morphology of 70 wt%BaSrTiO <sub>3</sub> /polyimide composite at ×10k of magnification of SEM equipmen .....	51
Figure 5.15 Morphology of 90 wt%BaSrTiO <sub>3</sub> /polyimide composite at ×10k of magnification of SEM equipment.....	52
Figure 5.16 Morphology of 95 wt%BaSrTiO <sub>3</sub> /polyimide composite at ×10k of magnification of SEM equipment.....	53
Figure 5.17 Thermogram of 70wt% BaSrTiO <sub>3</sub> /polyimide composite and pure polyimide at N <sub>2</sub> atmosphere .....	55
Figure 5.18 Dielectric properties between untreated and various silane treated BaSrTiO <sub>3</sub> /polyimide composite at 100 kHz .....	59
Figure 5.19 Dielectric properties various frequency of AEPTS silane treated BaSrTiO <sub>3</sub> /polyimide composite.....	60
Figure 5.20 Polarization of dipole material.....	61
Figure 5.21 Morphology of APTS silane treated filler.....	62
Figure 5.22 Morphology of APTS silane treated SrTiO <sub>3</sub> /BaSrTiO <sub>3</sub> /polyimide hybrid composite at 97%wt of overall filler contents.....	63
Figure 5.23 Side section morphology of APTS silane treated SrTiO <sub>3</sub> /BaSrTiO <sub>3</sub> /polyimide hybrid composite at 97%wt of overall filler contents .....	64
Figure 5.24 Dielectric properties of APTS silane treated SrTiO <sub>3</sub> /BaSrTiO <sub>3</sub> /polyimide hybrid composite at 97%wt of overall filler contents.....	65
Figure A1 FTIR spectra of untreated BST/PI composites.....	75
Figure A2 FTIR spectra of treated APTS BST/PI composites.....	76
Figure A3 FTIR spectra of treated AEPTS BST/PI composites.....	77
Figure A4 FTIR spectra of treated AEEPTS BST/PI composites .....	78
Figure A5 FTIR spectra hybrid of treated APTS SrTiO <sub>3</sub> /BST/PI composites.....	79
Figure B1 3D image of embedded capacitor before casting.....	80
Figure B2 3D image of embedded capacitor before casting2.....	81

	<b>Page</b>
Figure C1    Size distributions of BST particles.....	82
Figure C2    Size distributions of SrTiO <sub>3</sub> particles.....	83

# CHAPTER I

## INTRODUCTION

Electronic devices consist of passive components and active components. The main difference between active and passive components is that active ones require to be powered in some way to make them work and active components can also be used to amplify signals [1], more than 60-70% of the total area of the printed circuit board (PCB) is replaced by passive components. However, the main problem of passive components is its consumption of large area of the substrates to support it [1]. In recent years, embedded passive component was developed to solve this problem [2]. Embedded passive components (including resistor, capacitor and inductor) can be integrated into substrates, which are important for the next-generation electronic devices [11]. It has many advantages over past components, such as minimizing the spacing between chips and passives component, freeing more space on printed circuit board(PCB) and lowering the assembly cost and time for assembly each part [3].

Polymer/ceramic composites are the main ingredient for embedded capacitor, that consists of ceramic particles dispersed in the polymer matrix [4]. The good composite for embedded capacitor should have the following properties, high dielectric constant, low dielectric loss, high thermal stability and low cost. Polymer/ceramic composites are candidates for embedded capacitor because combine the low processing temperature of polymers and high dielectric constant of ceramics [5]. The interesting materials for embedded capacitors such as barium titanate( $\text{BaTiO}_3$ ), strontium titanate( $\text{SrTiO}_3$ ), barium strontium titanate ( $\text{BaSrTiO}_3$ ), strontium bismuth tantalite( $\text{SrBi}_2\text{Ta}_2\text{O}_9$ ), aluminum oxide( $\text{Al}_2\text{O}_3$ ), etc.

Barium strontium titanate( $\text{BaSrTiO}_3$ ) has been widely used as the ceramic filler in capacitor application, because of its high dielectric constant, low dielectric loss and low leakage current [6]. As another advantage, the synthesis method can get the small size particles of barium strontium titanate, that can improve various properties, such as high dispersibility, high purities, homogeneity, and better dielectric properties. Barium strontium titanate ( $\text{BaSrTiO}_3$ ) composed of solid solution of

strontium titanate( $\text{SrTiO}_3$ ) and barium titanate( $\text{BaTiO}_3$ ) in perovskite structure [7]. The dielectric of barium strontium titanate is 1000 or more as bulk and low range of 200-800 as for thin film [7].

As an organic, polyimides are mostly utilized polymer/ceramic composite in embedded capacitor applications, due to its credible good mechanical strength, high temperature stability, high flexibility, and good chemical stability [3]. It was, therefore, of interest to see if ceramic nanoparticles can be dispersed in the PI matrix to make superior nanocomposite integrated capacitors.[3] Polyimide can be prepared from the reaction of aromatic dianhydrides and diamines by one-step and two-step methods polymerization [9].

The main problems of polymer/ceramic composites are an agglomeration of ceramic particles in polymer matrix, resulted in poor dielectric properties of composites. From this problem, surface modification of nanoparticles is very important in order to prevent the aggregation of nanoparticles and enhance particle/polymer matrix interfacial interaction. [10] Silane treatment is one of the interesting techniques because silane coupling agents combine two different properties between inorganic group of the ceramic particles and organic group of the polymer by hydrolysis reactions. This process was used for decreasing aggregation and improved dispersion of ceramic particles in polymer matrix.

In this study, to increase the dielectric constant of the composites, barium strontium titanate particles were used filler in polymer matrix of the polyimides. Moreover, the comparison between the different effects of unimodal and bimodal system of barium strontium titanate( $\text{BaSrTiO}_3$ ) with strontium titanate( $\text{SrTiO}_3$ ) upon dielectric constant was performed. Barium strontium titanate( $\text{BaSrTiO}_3$ ) particles were surface modified with three kinds of silane coupling agents. The barium strontium titanate/ polyimide composites were characterized for morphology, dielectric and thermal properties.



## **1.1 The objectives of this thesis**

To increase the dielectric constant of the barium strontium titanate/ polyimide composites by using the different size, nano particle of barium strontium titanate and micro particle of strontium titanate.

To study the effect of surface modification by using the difference types of silane coupling agents on dielectric constants of barium strontium titanate filled polyimide composite.

## **1.2 The scope of this thesis**

- 1.2.1 To synthesize poly(amic acid) from 4,4'-oxydianiline (ODA) and pyromellitic dianhydride (PMDA) by using two-step polymerization method.
- 1.2.2 To investigate various weight fractions of barium strontium titanate, which were added into the polyimide matrix.
- 1.2.3 Two different particle sizes of barium strontium titanate and strontium titanate were studied and the effects of unimodal and bimodal barium strontium titanate powder on dielectric constant were investigated.
- 1.2.4 To improve the dispersion of barium strontium titanate in polyimide matrix by three different types of silane coupling agents such as 3-aminopropyltrimethoxysilane(aminosilane), 3-(2-Aminoethylamino) propyldimethoxymethylsilane and 3-[2-(2-Aminoethylamino)ethylamino]propyltrimethoxysilane.
- 1.2.5 To characterize barium strontium titanate/polyimide composite by using LCR meter, SEM, FT-IR, XRD, TGA and Tensile strength

## **1.3 Benefits of the thesis**

- 1.3.1 To develop barium strontium titanate/polyimide composite which use as embedded capacitor for electronic industry.
- 1.3.2 Developing the dielectric properties of polyimide composites by barium strontium titanate as ceramic filler.
- 1.3.3 Understanding the effect of dielectric constant on the barium strontium titanate/polyimide composite.

## CHAPTER II

### THEORY

#### 2.1 POLYIMIDE

During 1950s and 1960s, polyimide synthesis method has improved to a modern polyimide synthesis method by Edwards and Robinson at DuPont companies. Polyimide is a condensation polymerization polymer of imide monomers in their repeating units, as shown in Figure 2.1.

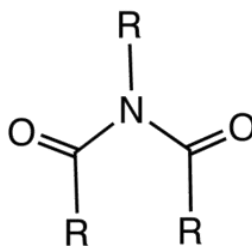


Figure 2.1 Structure of imide

The polyimides are normally derived from the reaction of organic tetracarboxylic acids and organic diamines or derivatives. The structure of the polyimide repeat unit was shown in Figure 2.2.

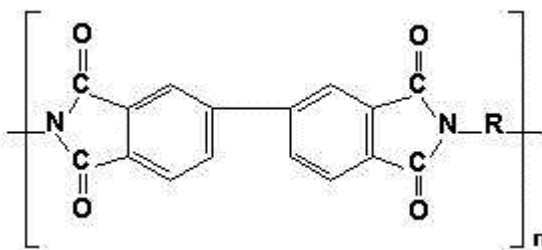


Figure 2.2 Polyimide Repeat Unit

In recent year, polyimides are normally used in industry, because of their good thermal stability, good chemical resistance, excellent mechanical properties and high tensile strength. The polyimides have attracted attention of users, so they are

applied in many applications, such as insulating film, microelectronics components, solar cell substrates, multilayer substrates, automotive and packaging industries. The general properties of polyimide can be shown in table 2.1.

Table 2.1 The properties of general polyimide [11].

Property	Comments
Thermosetting	commercially available as uncured resins, polyimide solution, laminates, thin sheets, stock shapes and machined parts
Thermoplastic	very often called <i>pseudothermoplastic</i> [11]
Crystalline	semi- crystalline or Amorphorous polymer Kapton Polyimide
Density	1.42 g/cm <sup>3</sup>
Max. Temperature	260 °C
Operating	
Flexural Modulus	2.48 GPa

## 2.2 Polyimide synthesis

There are two main methods to synthesize polyimide, namely one-step and two-step methods.

### 2.2.1 One-Step Method

In one-step method is commonly used when working with soluble polyimides that is soluble in organic solvents at polymerization temperatures. This method is started by heating a stoichiometric mixture of monomers in a high boiling point solvent at 140-250 °C. Phenolic solvents were usually used for the preparation of one-step method. Other successful solvents used at high temperatures were nitrobenzene,  $\alpha$ -chloronaphthalene and N-Methyl-2-pyrrolidinone [8]. Generally one-step method

used co-solvent, toluene, to removal water from condensation reaction. More phenolic solvents can be shown in table 2.2.

**Table 2.2** Typical phenolic solvents [8]

---

phenol
p-chlorophenol
m-cresol
p-cresol
2,4-dichlorophenol
o-chlorophenol

---

When the polyimide is soluble in organic solvents at polymerization temperatures, it is possible to react dianhydrides and diamines by using one-step polymerization methods in which polycondensation and imidization occur in the homogeneous solution. Alternatively, a solution of poly(amic acid) which has been allowed to equilibrate in a suitable solvent can be subsequently heated for cyclodehydration to soluble polyimide [10].

The advantages of soluble amorphous polyimides include the following[10];

- (1) the reaction requires only a single step: homogeneous solution imidization.
- (2) usually fewer than 1% of the amic-acid groups remain unimidized.
- (3) polyimides are hydrolytically stable compared to poly(amic acid)s and, therefore, may be stored under ambient conditions for long periods of time.
- (4) polyimide solids may be dissolved in polar solvents suitable for spin casting films.
- (5) when heat processing films, there is no release of water to form voids and cause shrinkage.

### 2.2.1 Two-Step Method Polymerization Via Poly(amic acids)

In two-step method polymerization is the most widely used procedure in polyimide synthesis. This method is consisted of two steps, firstly to prepare a soluble poly(amic-acid) which was then converted to the desired polyimide in the second step. The poly(amic acid) can be prepared by reaction of a diamine and a dianhydride at ambient condition in dipolar, aprotic solvent such as N,N-dimethylformamide (DMF), N,N-dimethylacetamide(DMAc) or N-Methylpyrrolidinone(NMP) to yield the corresponding poly(amic acid) intermediate at ambient temperature. A listing name of polyimide monomers are shown in table 2.3. The poly(amic acid) formation is completed within 24 h or less, depending on monomer reactivity. Films of poly(amic acid) can be prepared by casting a mixture solution of poly(amic acid) directly on a glass or metal substrate and then evaporated out the solvent by vacuum drying at 80 °C. After that the poly(amic acid) films are further cyclodehydration reaction (imidization) completely by thermal imidization or chemical imidization. Main advantages of this method over the one-step polymerization are the use of less toxic solvents and direct processing of the soluble poly(amic acid)s to form the final polyimide products such as films and fibers after imidization. Two-step method polymerization of polyimide can be shown in Figure 2.3.

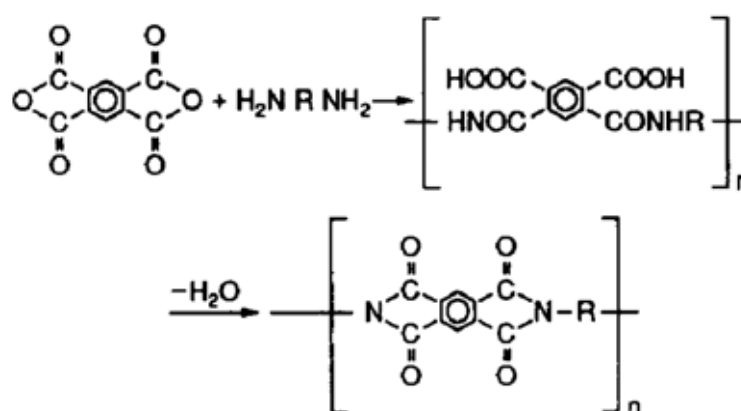


**Figure 2.3** Two-step method polymerization polyimide synthesis [8]

Table 2.3 Polyimide monomers [8]

Diamines	
<i>p</i> -phenylene diamine	PPD
<i>m</i> -phenylene diamine	MPD
4,4'-methylene dianiline	MDA
2-chlorophenylene diamine	CIPPD
benzidine	Bz
2,2'-dichlorobenzidine	2,2'-diClBz
3,3'-dimethylbenzidine	3,3'-diMeBz
4,4'-diaminodiphenyl ether	ODA
4,4'-diaminobenzophenone	4,4'-DABP
3,3'-diaminobenzophenone	3,3'-DABP
4,4'-diaminodiphenyl sulfone	4,4'-SO <sub>2</sub> D
4,4'-diaminodiphenyl sulfide	SDA
1,4-bis-(4-aminophenoxy)benzene	APB 4-1,4
1,4-bis-(3-aminophenoxy)benzene	APB 3-1,4
1,3-bis-(4-aminophenoxy)benzene	APB 4-1,3
1,4-phenylindane diamine	DAPI
2,2-bis-[4-(4'-aminophenoxyphenyl)] hexafluoropropane	4-BDAF
1,1-bis(4-aminophenyl-1-phenyl-2,2,2 trifluoroethane	3FDAM
2,2-bis(4-aminophenyl)hexafluoropropane	<i>p,p'</i> -6FDAM
2,2'-di-bis(trifluoromethyl)benzidine	PFMB <sup>a</sup>
3,5-diaminobenzotrifluoride	DABF <sup>b</sup>
Dianhydrides	
pyromellitic dianhydride	PMDA
3,3',4,4'-benzophenonetetracarboxylic dianhydride	BTDA
3,3',4,4'-biphenyltetracarboxylic dianhydride	BPDA
3,3',4,4'-oxydiphthalic anhydride	ODPA
4,4'-hexafluoroisopropylidenebis(phthalic anhydride)	6FDA
4,4'-bis(3,4-dicarboxyphenoxy) diphenylsulfide dianhydride	BDSDA
3,6-diphenylpyromellitic dianhydride	DPPMDA <sup>a</sup>
1,4-phenylenebis-(phenylmaleic anhydride)	1,4-P(PMA) <sup>c</sup>
4,4'-(1-phenyl-2,2,2-trifluoroethylidene bis(phthalic anhydride)	3FDA <sup>c</sup>
4,4',5,5'-dioxydiphthalic anhydride	DODPA <sup>d</sup>
4,4',5,5'-sulfonyldiphthalic anhydride	DSO <sub>2</sub> DA

<sup>a</sup> Research product: F. W. Harris, University of Akron.

<sup>b</sup> Occidental Chemical Co., Grand Island, NY, R. Buchanan.

<sup>c</sup> Research product: Amoco Chemical Co., Naperville, IL, E. K. Field.

<sup>d</sup> Research product: Occidental Chemical Co., Grand Island, NY, J. Stults.

<sup>e</sup> Research product: W. Alston, NASA Lewis.

### 2.3 Barium strontium titanate

Barium strontium titanate ( $\text{Ba}_x\text{Sr}_{1-x}\text{TiO}_3$ , BST) often referred as BST, is a mixed solid solution of barium titanate ( $\text{BaTiO}_3$ ) and strontium titanate ( $\text{SrTiO}_3$ ) in the perovskite structure, which is the most widely used material for electronic ceramics, because of excellent dielectric constant, small dielectric loss, low leakage current, low temperature coefficient of electrical properties, spontaneous polarization, below temperature and high compatibility with device processes. The dielectric of bulk barium strontium titanate is 1000 or more and that for thin film is in the low range of 200-800 [7]. The Barium strontium titanate has attracted attention of users, so it is applied in many applications, such as filled polymer, microwave components, implanted medical devices, aerospace components, standard capacitors. Barium strontium titanate has the perovskite structure which is shown in Figure 2.4.

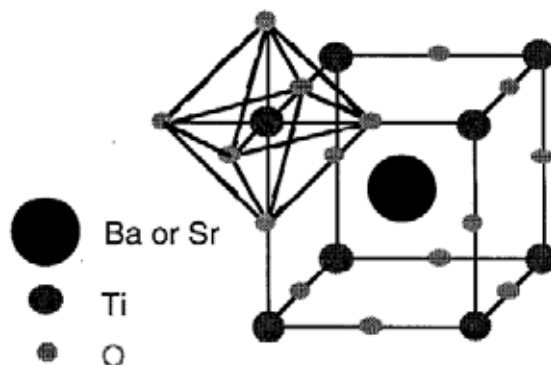


**Figure 2.4** Perovskite structure of barium strontium titanate [12]

In general, the electrical properties of barium strontium titanate ceramics were depended on the structure of perovskite. Tetragonal phases were evident ferroelectric properties with polarization hysteresis loop while paraelectric properties without polarization hysteresis loop were characteristics of cubic structure. Moreover, a brief summary of various properties of the two crystal structure is given in table 2.4.

**Table 2.4** The ferroelectric and paraelectric properties of perovskite materials [13]

<b>Property</b>	<b>Ferroelectric properties</b>	<b>Paraelectric properties</b>
Temperature	Below Curie temperature	Upper Curie temperature
Symmetric	Non-centrosymmetric	Centrosymmetric
Structure	e.g. Tetragonal phase, orthorhombic and rhombohedral	Cubic phase
Hysteresis	With hysteresis	Without hysteresis
Polarization	Spontaneous polarization	No spontaneous polarization
Electrical properties	Higher dielectric and higher dielectric loss	High dielectric and lower dielectric loss

Barium strontium titanate has a paraelectric properties, its lattice structure is cubic phase above the Curie point,  $T_c$ . And below the Curie point, it transforms successively to ferroelectric state, its lattice structure is tetragonal phase, as shown in Figure 2.5(a) [14]. When the temperature of material is above the Curie temperature, it displays the highly desirable nonhysteretic electric field response. Another important phenomenon related to this phase change is an increase in the temperature dependence of the relative permittivity, or dielectric constant, in the neighborhood of  $T_c$ , as shown in Figure 2.5(b) [14].

Additionally, different compositions of strontium ion modifies on barium strontium titanate have been proposed in order to improve the dielectric properties, i.e., the dielectric constant, the loss tangent, and tunability, along with the corresponding dependencies of these properties on temperature and on frequency.



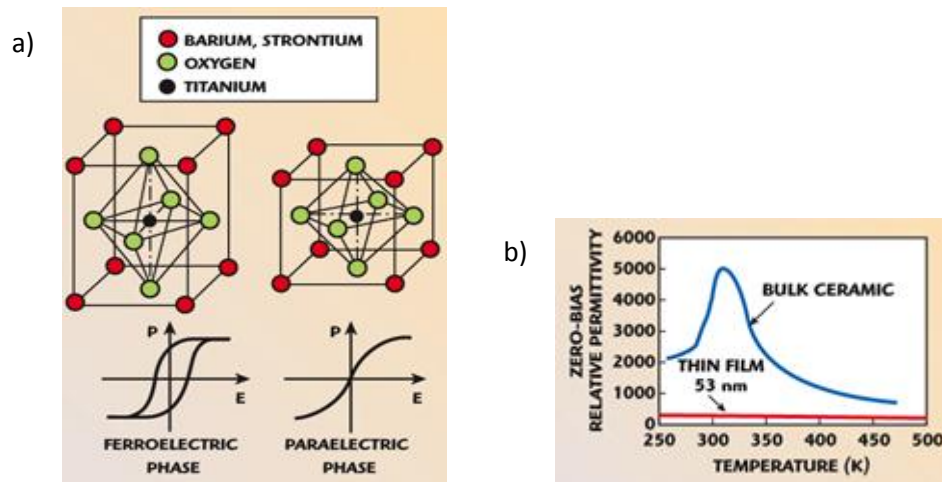


**Figure 2.5** a) Ferroelectric and paraelectric phases of BST b) temperature dependence of the relative permeability of thick and thin films of BST. [14]

Preparation of barium strontium titanate was synthesized by various techniques such as a solid state reaction [15], hydrothermal method [16], and sol-gel process [17]. The sol-gel method is the most commonly synthesized method for barium strontium titanate because of product's chemical homogeneity, high purity, fine crystalline size, and precise stoichiometry controls on the barium strontium titanate nanoparticles.

In this process, a solution, typically a solution of metal-organic compounds or a “sol”, a suspension of very fine particles in a liquid, is converted into a “gel”, a highly viscous mass. The simple flow chart of a sol-gel method was started from a suspension of fine particles (particulate or colloidal gel) and a solution (polymeric gel) as shown in Figure 2.6. [18]



The chemical reactions, which occurred during the conversion of the metal precursor solution to the gel, have a significant influence on the structure and chemical homogeneity of the gel. Foreign species such as counter ions, solvent molecules or chemical additives are often involved in the sol-gel chemistry. The rates of the chemical reactions are controlled by the processing variables such as chemical composition of the precursor, concentration of reactants, pH of the solution, and temperature. When the hydrolysis rate is of the same order of magnitude, or lower, than the condensation rate, precipitates or colloidal gels are usually obtained. High concentration of the precursor can also lead to precipitation.

## **2.4 Strontium titanate**

Strontium titanate ( $\text{SrTiO}_3$ ) is a mixed oxides compound of strontium and titanium. It has paraelectric properties with a perovskite structure at room temperature. In general, strontium titanate is stable at room temperature in cubic structure and transformation to tetragonal phase at temperature less than 105 K. At very low temperatures, strontium titanate shows piezoelectric and superconducting characteristics. The structure of strontium titanate has shown in Figure 2.7.

Strontium titanate is widely used material for electronic ceramics because of its high dielectric constant, high thermal stability, good mechanical strength, low coefficient of thermal expansion, high melting temperature and high chemical stability [19]. Nevertheless, strontium titanate have been widely used in a variety of applications, especially in electric equipments such as dynamic random access memory (DRAM), microelectronics, photoelectronics, microwave devices, solar and sensor technology.

In general, the strontium titanate particles can be prepared by solid-state reaction at a temperature range between 900 and 1000 °C. The various methods were used for synthesis of strontium titanate, such as sol-gel technique, hydrothermal method, precipitation method and combustion routes.

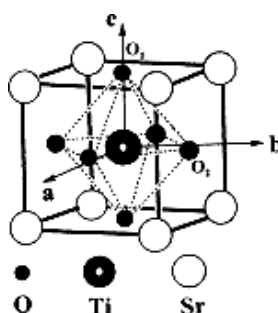


**Figure 2.7** General structure of strontium titanate [19]

**Table 2.5** Typical properties of strontium titanate [20-21]

Property	Value
Molecular formula	$\text{SrTiO}_3$
Structure Option	Perovskite
Molar mass	183.49 g/mol
Density	$5.19 \text{ g/cm}^3$
Melting point	$2080 \text{ }^\circ\text{C}$
Refractive index	2.41

## 2.5 Silane coupling agent

Silane coupling agent was used for the improvement of the mechanical properties of filled thermosetting and thermoplastic resins since the late 1940's [22]. It has the ability that from chemical links between organic and inorganic materials, as shown in Figure 2.8 [23]. The surface modified was generated to incorporate the bulk properties of heterogeneous environments of different phases into a uniform composite structure [23].

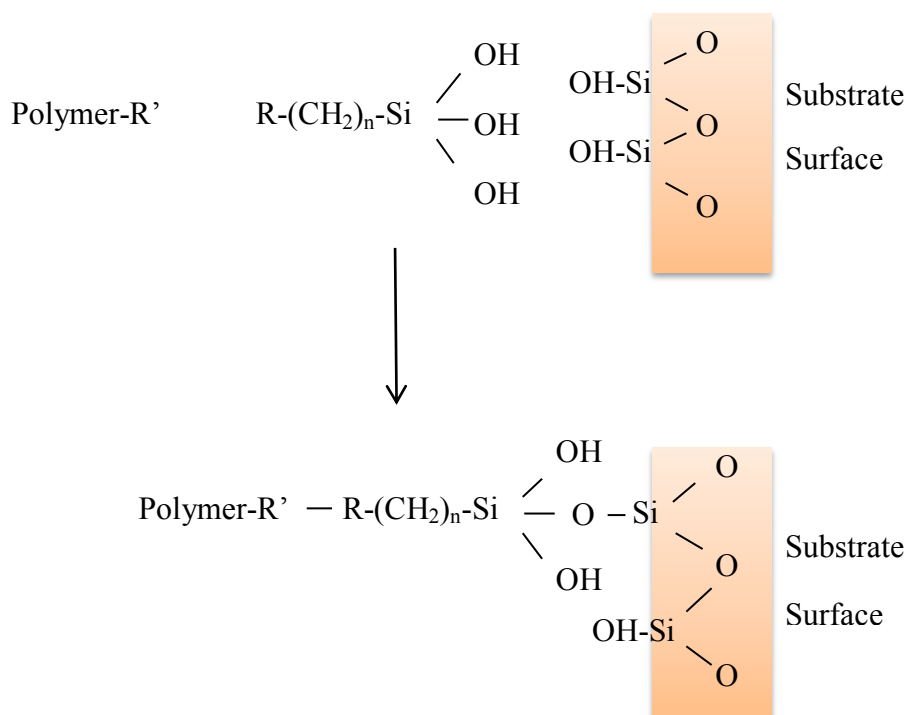


**Figure 2.8** Reaction of silane coupling agents to form chemical links between organic and inorganic materials. [23]

The general structures of the silane coupling agent are consisted of the two functionalities, such as shown in Figure 2.9. The first is a hydrolysable group such as alkoxy, acyloxy, halogen, and amine, respectively. Following hydrolysis, a reactive silanol group is formed, which can condense with other silanol groups to form siloxane linkages. Stable condensation products are also formed with other oxides such as those of aluminum, tin, zirconium, nickel and titanium [23]. The second group is a nonhydrolyzable organic radical that may possess a functionality that imparts desired characteristics.



## 2.6 Capacitor

A capacitor is a passive electronic component that stores energy in the form of an electrostatic field. In its simplest form, a capacitor consists of two conducting plates separated by an insulating material called the dielectric material. This material can be anything such as air, oil, paper, ceramic, mica etc. The dielectric material can increase the capacitance of the capacitor. A capacitor was showed in Figure 2.11

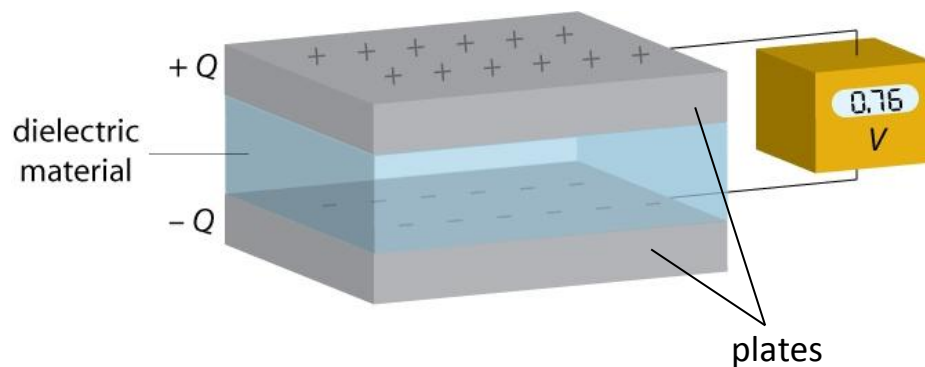


**Figure 2.11** The structure of capacitor [39]

When voltage is applied to the capacitor plates, an electric field is generated between them causing a significant difference of free electrons to develop between the capacitor plates. Free electrons are forced to gather on the negative connected plate and from the positive connected plate free electrons are taken away. This is the representation of the charge effect of the capacitor. The greater number of electrons polarized, the greater field generated and the greater charge of the capacitor. When the capacitor is disconnected from the power supply, it will remain charged. An ideal capacitor would remain charged indefinitely but in practice this is not possible due to a slight leakage current that is caused between the capacitor plates [40].

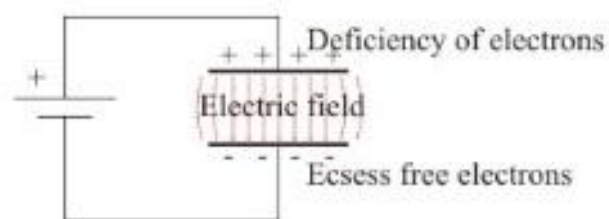


**Figure 2.12** The capacitor is applied the currents in system [40]

## CHAPTER III

### LITERATURE REVIEWS

**Burtrand I Lee et al.** in 2005[1] investigated the preparation of the thin BaTiO<sub>3</sub>/polyimide nanocomposite films with varying amounts of ceramic filler content by using a simple method in order to investigate its dielectric properties. By their method, firstly they prepared the BaTiO<sub>3</sub> powder by mixing between BYK-W9010 (copolymer) in NMP and BT-08 (ceramic filler), followed by ball milling for 15 h. The poly (amic acid) solution made from 3,3',4,4' benzophenone tetracarboxylic dianhydride and 4,4'-oxydianiline has been successfully prepared by using n-methyl pyrrolidinone as the common solvent. The BaTiO<sub>3</sub> slurry was added to poly (amic acid) solution with BaTiO<sub>3</sub> contents in the films varied from 30 to 90 %. Lastly, films on glass substrate were made by spin coating technique. The composites exhibited a low weight loss and were stable above 300°C but started to degrade at about 325 – 350°C. The amorphous composites have no undesirable interaction at the interface of BaTiO<sub>3</sub> – Polyimide. The high dielectric properties at 125 at frequency of 1 kHz with a specific capacitance of 28.4 nF/cm<sup>2</sup> for 90 vol % of BaTiO<sub>3</sub> content was achieved. These composites exhibited the stable dielectric constants in the frequency range from 1 kHz to 1 MHz.



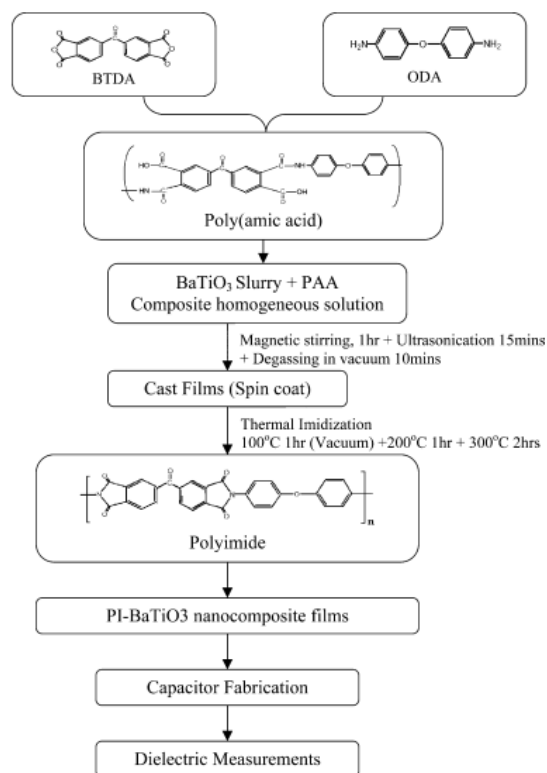


**Figure 3.1.** Flow sheet explains the fabrication of ceramic-polymer nanocomposites. [1]

**Bao-Ku Zhu et al.** in 2005[4] investigated the films' preparation and properties of polyimide/LTNO composite with high dielectric constant. The polyimide/LTNO composite films were prepared by using a colloidal process. In this process, Li and Ti doped NiO (LTNO) particles were dispersed into poly(amic acid) solution. The LTNO powder with particle size of 100  $\mu\text{m}$  was synthesized by sol-gel technique. LCR electrometer, thermal – gravimetric analyses (TGA) and X-ray diffraction (XRD), scanning electron microscope (SEM) were used for characterization of the dielectric properties, thermal properties and structures of the obtained composites. The dielectric constants and conductivity of the composites were the weak temperature dependence in the ranges from 30°C to 150°C but they could be increased by increasing the volume fraction of LTNO. The composites showed high thermal stability with decomposition temperature of 5% weight loss above 500°C in all samples.

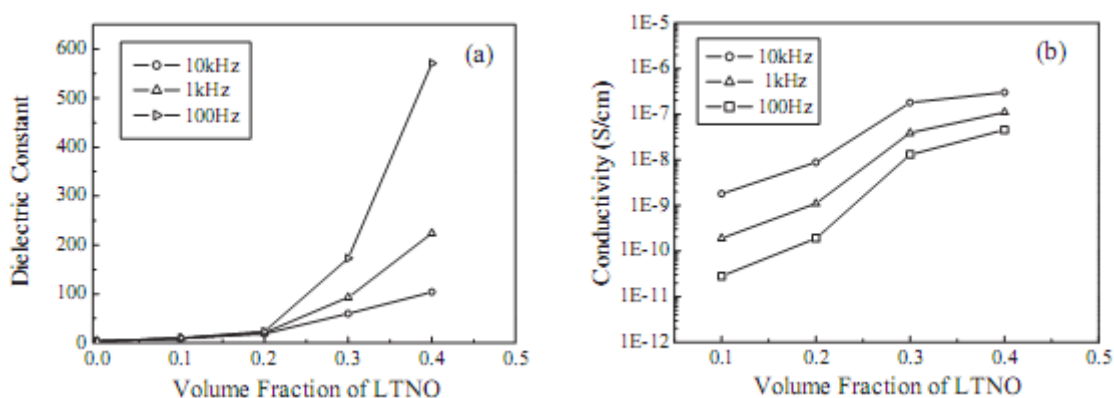


**Figure 3.2** Dependence of (a) dielectric constant and (b) electrical conductivity of the PI/LTNO composite films on the volume fraction of LTNO at different frequencies (at 30°C). [4]

**Seung-Hoon Choi et.al** in 2006[26] reported the effect of coupling agents with different organic moiety on the dielectric properties of polyimide/BaTiO<sub>3</sub> composite films. INAAT (isopropyl tris(N-amino-ethyl-aminoethyl)titanate, KR44) and APTS (3-amino-propyl-triethoxysilane) were used as coupling agents, respectively, for homogeneous dispersion of BaTiO<sub>3</sub> particles into a polyimide matrix. The preparation consisted of three steps. Firstly, the barium titanate (BaTiO<sub>3</sub>) was treated with APTS or INAAT. Secondly, the step of synthesis poly(amic acid) based on PMDA(pyromellitic dianhydride) and ODA (4,4' – oxydianiline) was performed. Finally, the BaTiO<sub>3</sub>/polyimide composite films were prepared by homogeneously mixing the poly(amic acid) solution and the barium titanate slurry and spin casting to form films. The dielectric constant of the BaTiO<sub>3</sub>/PI composites films treated by APTS and INAAT as a function of the BaTiO<sub>3</sub> volume fraction were determined. The polyimide/INAAT-treated BaTiO<sub>3</sub> composite had a higher dielectric constant ( $\epsilon_r=19.03$ ) than that of the polyimide/APTS-treated BaTiO<sub>3</sub> composite ( $\epsilon_r=14.64$ ).

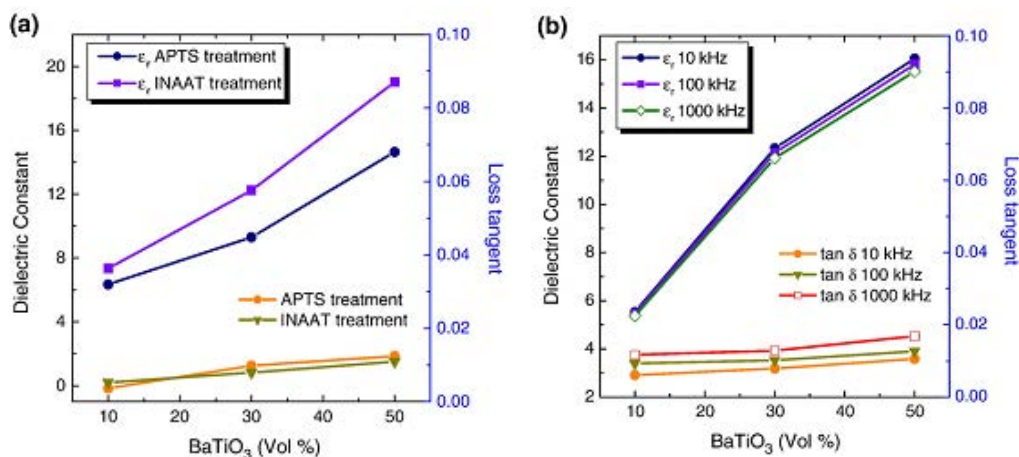


**Figure 3.3** (a) Dielectric constant and loss tangent as a function of loading volume of BaTiO<sub>3</sub> particles treated by INAAT and APTS coupling agents and (b) frequency dependence for dielectric constant and dielectric loss of the polyimide/INAAT-treated BaTiO<sub>3</sub> composite. [26]

**Hongyan Li et al.** in 2006[36] reported dielectric properties of polyimide/Al<sub>2</sub>O<sub>3</sub> hybrids synthesized by in-situ polymerization. The polyimide/nano-Al<sub>2</sub>O<sub>3</sub> composites were prepared by in-situ polymerization. Firstly, the step of synthesis polyimide by mixing PMDA and ODA (1:1 by mole) was performed, and then the Al<sub>2</sub>O<sub>3</sub> solution was prepared by mixing Al<sub>2</sub>O<sub>3</sub> and DMAc. Finally, Al<sub>2</sub>O<sub>3</sub>/PI hybrid film was prepared by homogeneously mixing the Al<sub>2</sub>O<sub>3</sub> solution with polyimide solution at room temperature. The mixture was cast on clean glass plates and cured at 150, 200 and 250°C for 1 hr., respectively. The results showed that the life time of the hybrid film with 20 wt% Al<sub>2</sub>O<sub>3</sub> loading was 10 times longer than that of the unfilled PI.

**Tao Hu et al.** in 2007[28] investigated the dielectric properties of BST/polymer composite. The loading effect of two different BST materials (Ba<sub>0.55</sub>Sr<sub>0.45</sub>TiO<sub>3</sub> with micrometer-scale particles and Ba<sub>0.5</sub>Sr<sub>0.5</sub>TiO<sub>3</sub> with nanometer-scale particles) on the dielectric properties and microstructures of the composite were studied. Firstly, the COC (cyclic olefin copolymer) polymer was mixed with the BST powders in the chamber of the Torque Rheometer at 230 °C, followed by hot-pressing at 200 °C to form samples for measurements. Composite

samples had a length and width of 20–30 mm and thickness of 1.5–2 mm. The results showed that the relative permittivity and losses of the composites increased as the volume fraction of BST powder was increased. The BSTn-COC composite with nanopowder showed higher relative permittivity and loss at BST loading over 10 vol.% compared with the common powder composites. Also the microstructures of the composites showed homogeneous distribution of the BST powders in the COC polymer matrix in all the samples.

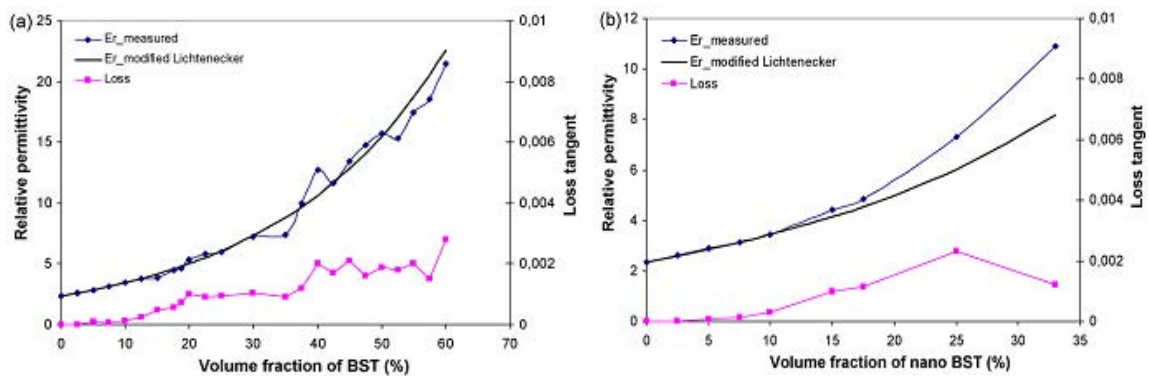


**Figure 3.4.** Relative permittivities and loss tangents of (a) the BSTc-COC composites and (b) the BSTn-COC composites at 1GHz as a function of BST loading. [28]

**M. Konno et al.** in 2007[29] investigated the fabrication and dielectric properties of the BaTiO<sub>3</sub>-polymer nano-composite thin films. The preparation consisted of two steps. Firstly, Metallic barium was used for synthesis of BaTiO<sub>3</sub> particles. Finally, BaTiO<sub>3</sub> – polymer nano-composites films were prepared by homogeneous mixing of the PVDF (polyvinylidene fluoride) or SPAI (siloxane-modified polyamideimide) in NMP and barium titanate and forming films by spin coating on glass substrate. The results showed that the root mean square roughness of the BaTiO<sub>3</sub> – PVDF composite film was less than 20 nm at a particle volume fraction of 30%. The 30 vol% BaTiO<sub>3</sub> – PVDF composites film exhibited a dielectric constant of 31.8 which was four times larger than of the pure PVDF films.

**Bhupendra K. et al.** in 2008[30] investigated the preparation and characterization of polyaniline–ZnO composite and its dielectric behavior. The preparation consisted of three steps. Firstly, polyaniline was synthesized by polymerization of aniline in the presence of hydrochloric acid (acts as a catalyst) using ammonium per-oxidisulphate (act as an oxidizing agent). Secondly, the zinc oxide (ZnO) powder was prepared by a sol-gel method,  $\text{Zn}(\text{Ac})_2 \cdot 2\text{H}_2\text{O}$  has been used as a main source for Zn. Finally, ZnO – PANI composites were prepared by homogeneous mixing the undoped polyaniline solution with ZnO composites and finally spin coating on glass substrate. Films were characterized by fourier transform infrared spectroscopy (FTIR), X-ray diffraction (XRD), scanning electron microscopy (SEM).

**F.J. Wang et al.** in 2010[31] investigated the preparation of the polyethersulfone (PES)/barium titanate ( $\text{BaTiO}_3$ ) composites using a colloidal process with hot-pressing method. In this process, the modified  $\text{BaTiO}_3$  particles were synthesized in polyether sulfone (PES) solution. Fourier transform infrared spectroscopy (FT-IR), X-ray diffraction (XRD), scanning electron microscope (SEM), thermal – gravimetric analyses (TGA) and LCR digital meter were used to characterize the dielectric properties, thermal properties and structures of the obtained composites. It was found that  $\text{BaTiO}_3$  particles with average size of 100 nm were dispersed in the structure of polyethersulfone matrix. The dielectric constant and the loss tangent of these composites increased when the volume fraction of  $\text{BaTiO}_3$  particles increased, but both values decreased if temperature and frequency increased. Moreover, the composites indicated the high glass transition temperature ( $>225^\circ\text{C}$ ) and 5.0 % weight loss at temperature ( $>500^\circ\text{C}$ ).

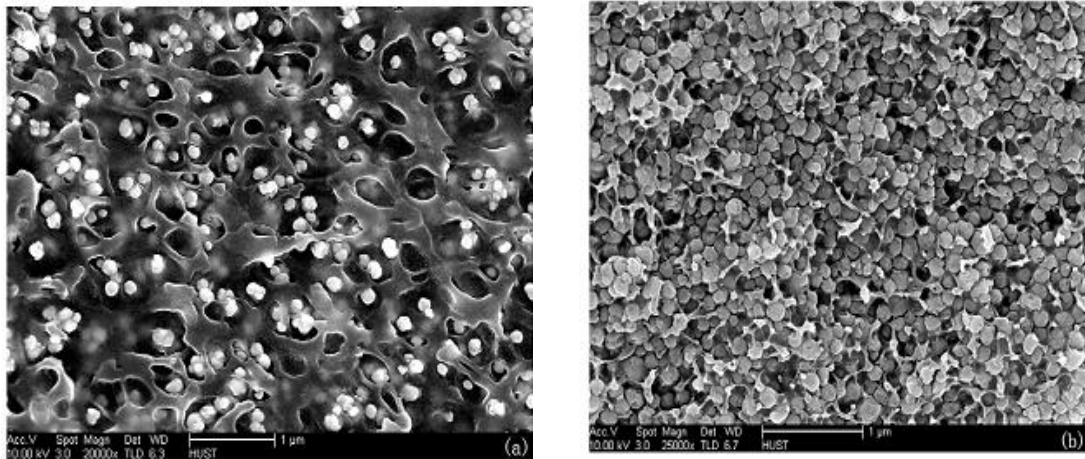


**Figure 3.5** SEM image of fractured cross surface of the BaTiO<sub>3</sub>-PES composites with BaTiO<sub>3</sub> volume fractions (a) 30% and (b) 50%. [31]

**Asliza A. et al.** in 2011[32] prepared the polyimide/Al<sub>2</sub>O<sub>3</sub> composite films in order to improve solid dielectrics. The preparation consisted of three steps. Firstly, the step of synthesis poly(amic acid) by PMDA(pyromellitic dianhydride) and ODA (4,4' – oxydianiline) was performed. Secondly, the alpha-alumina [ $\alpha$ - Al<sub>2</sub>O<sub>3</sub>] solution was prepared by dispersing Al<sub>2</sub>O<sub>3</sub> particles with an average size of 0.5  $\mu$ m in DMAc and stirred under ultrasonication for 3 h. Finally, polyimide/Al<sub>2</sub>O<sub>3</sub> composite were prepared by homogenous mixing the poly(amic acid) solution with Al<sub>2</sub>O<sub>3</sub> in DMAc solution, and then the solution was directly casted onto the glass dish. The films were characterized by Fourier transform infrared spectroscopy (FT-IR), X-ray diffraction (XRD), Scanning electron microscope (SEM) and LCR electrometer. The dielectric constant of the polyimide/Al<sub>2</sub>O<sub>3</sub> composite was higher than that of the polyimide film with the dielectric constant increased from 3 up to 6 with only 30 wt% of Al<sub>2</sub>O<sub>3</sub> loading at a frequency of 1 MHz.

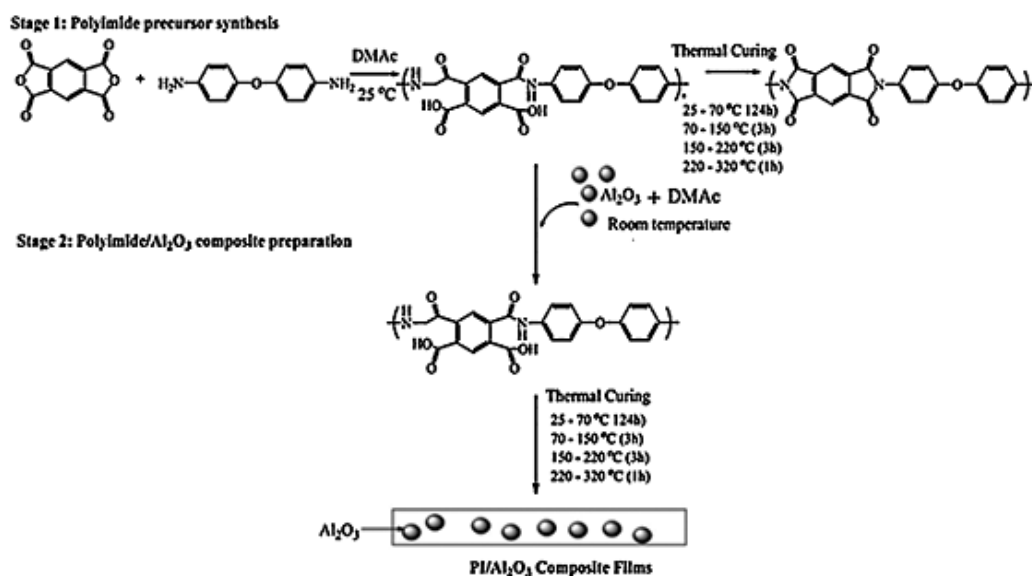


**Figure 3.6** Schematic of PI and PI/Al<sub>2</sub>O<sub>3</sub> composite film preparation and reactions involved in the process. [32]

**S.Dong Cho et al.** in 2004 [3] studied the dielectric constant of epoxy/BaTiO<sub>3</sub> composite as embedded capacitor films. The epoxy composite filled with nano and micro size particle of BaTiO<sub>3</sub> for comparison. The results showed that the dielectric constant of micro epoxy/BaTiO<sub>3</sub> composite was higher than nano epoxy/BaTiO<sub>3</sub> composite, and exhibited a maximum the dielectric constant of unimodal system composites is about 57 at 60 vol% of content of filler. The bimodal particles size of epoxy/BaTiO<sub>3</sub> composite was prepared by 60 vol.% of micro-sized BaTiO<sub>3</sub> and 15 vol.% of nano-sized BaTiO<sub>3</sub>. The maximum dielectric properties at 90 at frequency of 100 kHz with specific capacitance of 8 nF/cm<sup>2</sup> and leakage current of less than 1x10<sup>-7</sup> A/cm<sup>2</sup> occurred at 75 vol.% of bimodal BaTiO<sub>3</sub> content. X-ray diffraction (XRD), Scanning electron microscope (SEM), Differential scanning calorimeter (DSC) and LCR digital meter were used for characterization of the dielectric properties, thermal properties and structures of the obtained composites films.

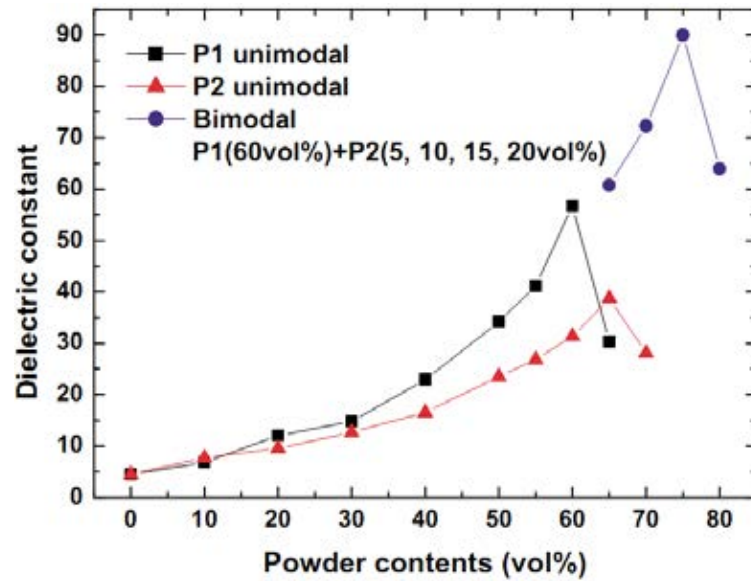


**Figure 3.7** Dielectric constant changes with BaTiO<sub>3</sub> powder loading. [3]

Kensaku Sonoda et al. in 2009 [33] studied the effect of surface modification on dielectric and mechanical properties of polypropylene-graft-poly(styrene-stat-divinylbenzene)/barium strontium titanate composite. The preparation consisted of two steps. Firstly, the particles of barium strontium titanate were treated with aliphatic carboxylic acid to enhance the compatibility between ceramic particles and the polymer matrix. Secondly, the composites were prepared by adding both the surface-modified barium strontium titanate and polypropylene-graft-poly(styrene-stat-divinylbenzene) into a small-scale twin-screw extruder at 215 °c. The results showed that the relative permittivity of the BST/ER composite modified by carboxylic acid was better than unmodified BST/ER composite. The maximum relative permittivity was about 18.31 at 1 GHz for the BST/ER composite treated by stearic acid. Tensile strength and Young's modulus of the modified and unmodified barium strontium titanate were similar.



## CHAPTER IV

### EXPERIMENT

#### 4.1 Materials and chemicals

1. Barium hydroxide octahydrate ( $\text{Ba}(\text{OH})_2 \cdot 8\text{H}_2\text{O}$ ) purchased from Sigma-Aldrich Chemical, Inc.
2. Strontium nitrate ( $\text{Sr}(\text{NO}_3)_2$ ) purchased from Sigma-Aldrich Chemical, Inc.
3. Sodium hydroxide ( $\text{NaOH}$ ) purchased from Sigma-Aldrich Chemical, Inc.
4. Titanium (IV) isopropoxide purchased from Sigma-Aldrich Chemical, Inc.
5. Strontium titanate ( $\text{SrTiO}_3$ ) purchased from Sigma-Aldrich Chemical, Inc.
6. 3-aminopropyltrimethoxysilane (APTS) purchased from Louis T. Leonowens(Thailand) Ltd.
7. 3-(2-Aminoethylamino)propyltrimethoxymethylsilane (AEPTS) purchased from Koventure Co., Ltd.
8. 3-[2-(2-Aminoethylamino)ethylamino]propyl-trimethoxysilane (AEEPTS) purchased from Sigma-Aldrich Chemical, Inc.
9. 4,4'-Oxydianiline (ODA) purchased from Fluka Company, Inc.
10. Pyromellitic dianhydride (PMDA) purchased from Sigma-Aldrich Chemical, Inc.
11. N-Methyl-2-pyrrolidinone (NMP) purchased from Merck KGaA Germany.
12. Methanol (Commercial grade) was purchased from SR lab.
13. Ethanol (Commercial grade) was purchased from SR lab.
14. Acetic acid purchased from Sigma-Aldrich Chemical, Inc.

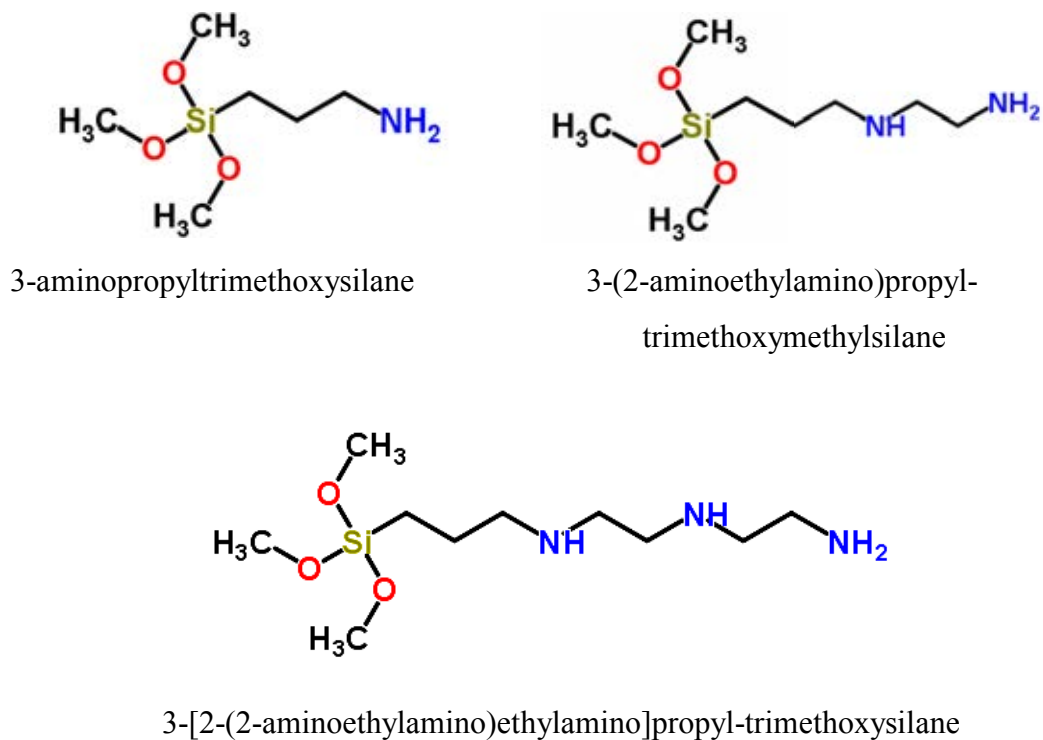


**Figure 4.1** Structures of three types of coupling agents

## 4.2 Equipments

### 4.2.1 Barium strontium titanate synthesis part

#### a) Centrifuge

A Centrifuge model ROTOFIX32 was used for separating liquid from solids. The maximum working rotation speed of this machine is 6000 RPM.



(Ref : [http://www.analytik.de/component/option,com\\_marketplace/page,show\\_ad/catid,4685/adid,16016/Itemid,914/](http://www.analytik.de/component/option,com_marketplace/page,show_ad/catid,4685/adid,16016/Itemid,914/))

**Figure 4.2** Centrifuge machin

### **b) Hot Plate and Magnetic Stirrer**

The magnetic stirrer and hot plate model RCT basic from IKA Labortechnik were used.

### **c) Chamber furnace**

A Carbolite CWF 1300 Chamber furnace was used in these experiments. The maximum operating temperature is 1300°C. The instrument was utilized for thermal treatment of the barium strontium titanate particles.



(Ref : [http://labcelcius.com/proddetail.asp?prod=cf\\_furnace\\_cwf](http://labcelcius.com/proddetail.asp?prod=cf_furnace_cwf) )

**Figure 4.3** Carbolite furnace

### **d) Syringe, Needle**

The syringe used in these experiments had a volume of 10, 5, 1 ml and the needle were No. 17 and 20, respectively.

## **4.2.2 Surface modification of barium strontium titanate particle part**

### **a) Cooling System**

The cooling system in the solvent distillation was needed in order to condense the freshly evaporated solvent from the reactor during the synthesis.

### (b) Ultrasonic

Ultrasonic (VGT-1860QTD) dispersing helped to improve the dispersion quality of the fillers.



**Figure 4.4** Ultrasonic

### 4.2.3 Preparation of polyimide/ barium strontium titanate composite part

#### a) Glove box

Glove box (Inert Atmospheres) with oxygen and moisture analyzer designed for handling solid reagents under inert atmosphere and for storing air-sensitive reagents. Inside the glove box, oxygen and moisture levels are normally controlled to below 0.1 ppm. The glove box is shown in **Figure 4.5**.



(Ref : <http://www.mse.engin.umich.edu/people/faculty/kim/facilities>)

**Figure 4.5** Glove box

### b) Vacuum oven

A Thermo scientific vacuum oven was used for removing solvent from freshly cast films and used for thermal treatment of the polyimide film. This vacuum oven can be programmed. All functions can be set from digital panel and can display their status on LCD. The temperature and pressure are controllable variables. The maximum working temperature of this machine is 500°C.



**Figure 4.6** Vacuum oven

### c) Temperature controlled oven

A Carbolite LHT5/30 (201) Temperature controlled oven was utilized in these experiments. The maximum working temperature of this machine is 500°C. The equipment was used for thermal treated the polyimide film.

## 4.3 Barium strontium titanate synthesis

Barium strontium titanate particles synthesized via sol-gel process. To a 100 mL two – neck flask, barium hydroxide octahydrate ( $\text{Ba}(\text{OH})_2 \cdot 8\text{H}_2\text{O}$ ) 3.95 g and strontium nitrate ( $\text{Sr}(\text{NO}_3)_2$ ) 2.65 g were added in sodium hydroxide (NaOH) 2.00 g and mixed with distilled water 42.5 mL as a solvent. Then, the reaction was prepared in a water bath with magnetic stirrer in order to heat the mixture solution to certain temperature for 1 h. After, cooling to room temperature by stirring, titanium (IV) isopropoxide liquid 7.5 mL was slowly loaded in the mixture solution. The solution was stirred at room temperature for 18 h. When the reaction was complete, the

mixture solution was washed with methanol three times by centrifugation. After that, the gel was heated by a heating oven in order to remove the residue solvent. The sample was calcined at 750°C by chamber furnace to obtain the barium strontium titanate particles.

#### 4.4 Surface modification of barium strontium titanate particles

Ethanol and deionized water were mixed in a laboratory flask and adjusted its pH to around 4-5 by acetic acid. The weight ratio of ethanol:deionized water was 9.5 : 0.5, respectively. The silane coupling agent was added into the solution flask and stirred at room temperature by magnetic stirrer to hydrolysis and formation of silanol.

The amount of suitable silane coupling agent was calculated by the equation below:[34]

$$\text{Amount of silane (g)} = \frac{\text{amount of filler (g)} \times \text{specific surface area of filler (m}^2\text{/g)}}{\text{wetting surface of silane (m}^2\text{/g)}}$$

Calculation of suitable silane coupling agent was important in order to obtain the mono-layer coverage of silane coupling agents upon the surface of barium strontium titanate particles.

After that, the barium strontium titanate fillers were added to the mixture solution and heated to reflux. After the solution was cooled to room temperature for 1 hr., and the particles were washed three times with absolute ethanol by filtration. The particles were dried in vacuum oven. Finally, after vacuum drying, the particles were grinded by mortar and pestle for 30-40 min to obtain the modified barium strontium titanate particles.

## **4.5 Preparation of polyimide/ barium strontium titanate composites**

### **4.5.1) Preparation of poly(amic acid)**

Poly(amic acid) was synthesized by using two-step polymerization method. The solid content and mole ratio of dianhydride:diamine were 15 wt% and 1:1, respectively. Firstly, both 4,4'-oxydianiline (ODA) and pyromellitic dianhydride (PMDA) were dissolved in N-Methyl-2-pyrrolidinone (NMP) as a solvent (approximately 4 ml solution). The mixture solution was stirred at room temperature for 1 h by magnetic stirrer to obtain poly(amic acid) solution.

### **4.5.2) Preparation of polyimide/ barium strontium titanate composite**

Appropriate amount of modified barium strontium titanate particles were added in 1 mL of N-Methyl-2-pyrrolidinone (NMP) solution and the mixed solution was stirred by magnetic stirrer. The solution was sonicated to ensure well dispersion. Then the poly(amic acid) solution was added to the mixed solution and the solution was stirred for 1 h by magnetic stirrer. The mixture solution was sonicated by ultrasonic machine. All of the composites were prepared by casting poly(amic acid)/barium strontium titanate solution on a glass substrate or the prepared circuit and were dried in vacuum oven. The composites were annealed at certain temperature in a heating oven to obtain polyimide/barium strontium titanate composites.

### **4.5.3) Preparation of polyimide/ barium strontium titanate embedded capacitor**

The embedded capacitor was prepared by casting the suspension solution of poly(amic acid)/barium strontium titanate to embedded capacitor substrates, as show in Figure 4.7 It was dried in order to remove NMP solvent in composite. The embedded capacitor was heat treatment at certain temperature in a heating oven to obtain polyimide/barium strontium titanate embedded capacitor.

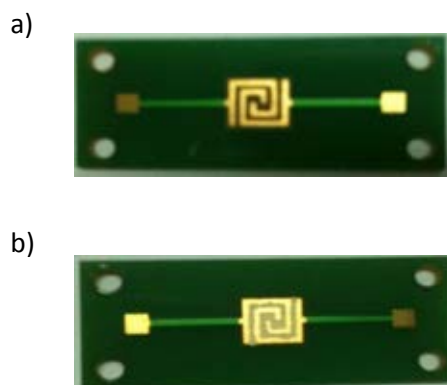


**Figure 4.7** Embedded capacitor of composite

a) before casting b) after casting

## 4.6 Characterization Instruments

### 4.6.1 Infrared Spectroscopy (FTIR)

Infrared spectra were recorded with Nicolet 6700 FTIR spectrometer. The scanning frequency ranged from 400 to 4000  $\text{cm}^{-1}$  with 64 times scanning. The functional groups of the composite films ( $1.5 \times 1.5 \text{ cm}^2$ ) were identified.



**Figure 4.8** Fourier transform infrared spectroscopy (FTIR) Equipment.



#### 4.6.2) Scanning electron microscope (SEM)

The morphologies of polyimide/ barium strontium titanate composites were investigated by SEM (Hitachi model S-3400N). The composites for SEM analysis were coated with platinum particles by ion sputtering device to provide electrical contact to the specimen.



(ref:<http://www.jeol.com/PRODUCTS/ElectronOptics/ScanningElectronMicroscopes>  
SEM/HighVacuumLowVaccum/JSM6510/tabid/524/Default.aspx)

**Figure 4.9** Scanning electron microscopy (SEM)

#### 4.6.3) Thermogravimetric Analysis (TGA)

The weight loss with temperature ramp was investigated by TGA. The temperature ranged from ambient to 1000°C and the scan rate was 10°C/min.



(ref :<http://www.sithiphorn.com/wordpress/?p=44>)

**Figure 4.10** Thermogravimetric analysis (TGA) equipment

#### 4.6.4) X-ray diffraction (XRD)

Crystalline phases of the product were determined from X-ray diffraction analysis, using a SIEMENS D5000 diffractometer with  $\text{CuK}\alpha$  radiation. Each sample was scanned in the range of  $2\theta = 10\text{-}50^\circ$  with a step size of  $2\theta = 0.02^\circ$ .

#### 4.6.5) LCR meter

The dielectric properties of composites were investigated by LCR meter, ranged from 1 kHz to 1 GHz.



(Ref ;<http://www.testequity.com/products/1404/>)

**Figure 4.11** LCR meter

#### 4.6.6) Transmission electron microscopy (TEM)

The morphology of an individual grain of the BST samples was observed by a JEOL JEM-2100 Analytical Transmission Electron Microscope, operated at 80-200 keV at the Scientific and Technological Research Equipment Center (STREC), Chulalongkorn University.

## CHAPTER V

### RESULTS AND DISCUSSION

This thesis was conducted in order to investigate the dielectric properties of polyimide/ barium strontium titanate(BST) composite for embedded capacitor application. In this chapter, the results such as thermal properties, electrical properties, and morphologies were described into three main sections. The characteristics of the barium strontium titanate(BST) synthesized by sol-gel method (I), surface modification of barium strontium titanate particles on composites (II) and hybrid composite of the SrTiO<sub>3</sub>/BaSrTiO<sub>3</sub>/polyimide (III) were described in section 5.1, 5.2 and 5.3 respectively.

#### 5.1 Barium strontium titanate synthesis

In this research, the barium strontium titanate particles were synthesized by sol-gel method. The reactions occurred in the sol-gel chemistry were the hydrolysis and the condensation reaction. This process was prepared from barium hydroxide octahydrate(Ba(OH)<sub>2</sub>.8H<sub>2</sub>O), strontium nitrate (Sr(NO<sub>3</sub>)<sub>2</sub>) and titanium (IV) isopropoxide. Sodium hydroxide(NaOH) and water were used as solvents in this methods. The synthesis product was then calcined under stag air at 750 °C. The structure of barium strontium titanate particles were investigated by X-ray diffraction (XRD), as shown in Figure 5.1.

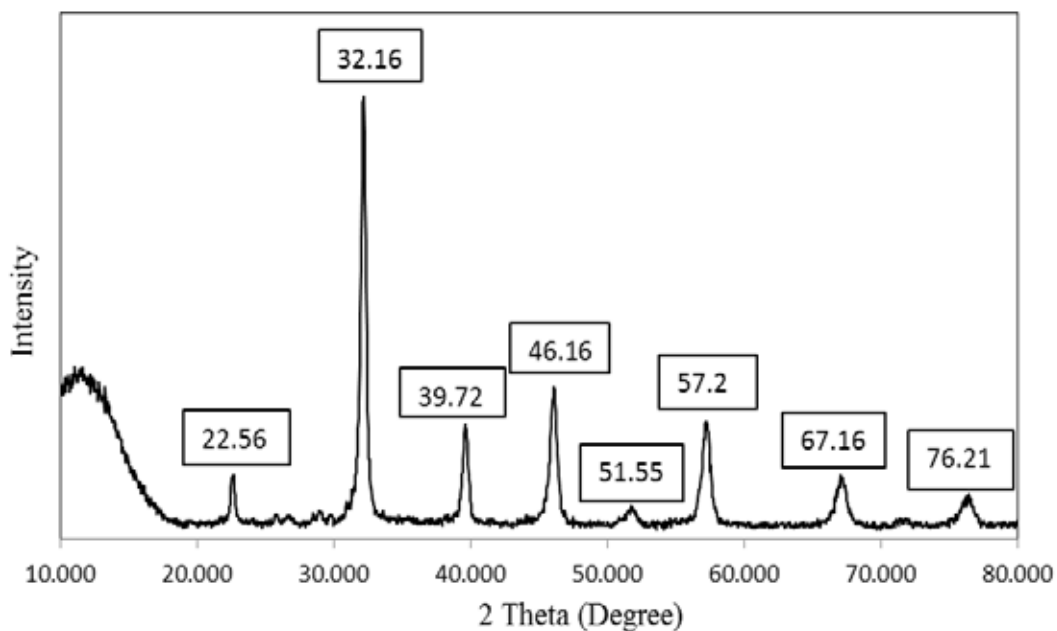


**Figure 5.1** The XRD patterns of barium strontium titanate.

Wong N.g. et al. reported that the synthesis nanocrystalline  $\text{Ba}_{0.5}\text{Sr}_{0.5}\text{TiO}_3$  powder by sol-gel method. The XRD peak of the barium strontium titanate stoichiometries ( $\text{Ba}_{0.5}\text{Sr}_{0.5}\text{TiO}_3$ ) were reported at  $22.49^\circ$ ,  $32.03^\circ$ ,  $39.50^\circ$ ,  $45.50^\circ$ ,  $51.75^\circ$ ,  $57.11^\circ$ ,  $67.01^\circ$ ,  $71.67^\circ$  and  $76.23^\circ$  respectively [35]. The comparison our result was showed in Figure 5.1. Similarly, both results were similar and confirmed perovskite structure of the barium strontium titanate particles. From the XRD curve, samples of barium strontium titanate were proven not to appear with common impurity, barium carbonate, in structure.

### 5.1.1 Particle size of barium strontium titanate

The particle size and morphology of barium strontium titanate particles were investigated by transmission electron microscopy (TEM) and scanning electron microscopy (SEM), as shown in Figure 5.2 and 5.3 respectively.

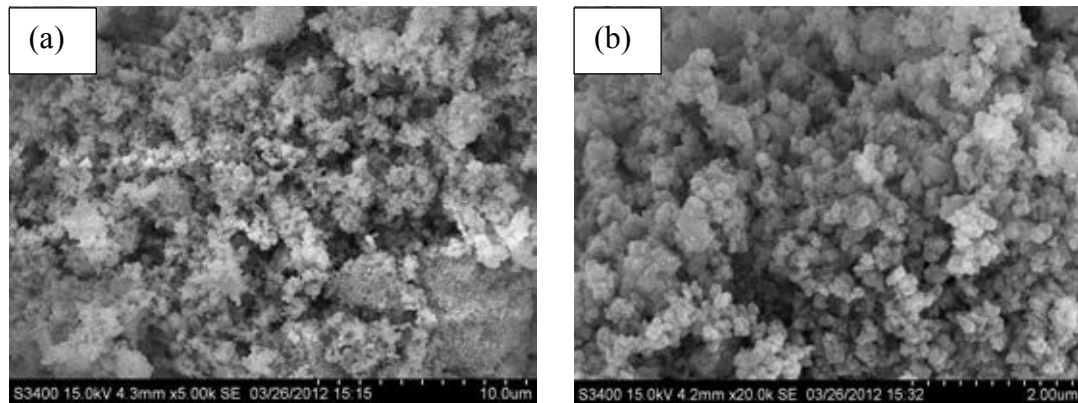


**Figure 5.2** SEM micrographs of barium strontium titanate particles at various magnification of SEM equipment a)  $\times 5k$ , b)  $\times 20k$

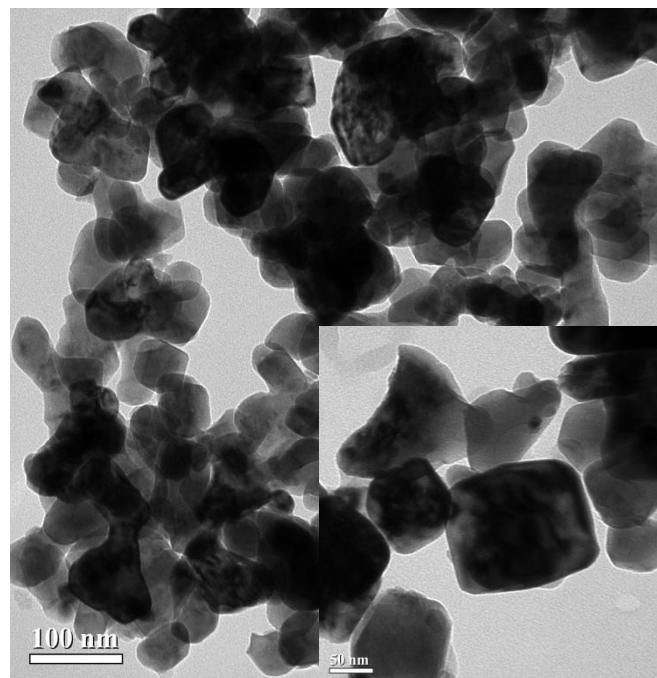


**Figure 5.3** TEM micrographs of barium strontium titanate particles.

In Figure 5.2 and 5.3, the particles size of barium strontium titanate was showed and exhibited small particles with some agglomerate from some small barium strontium titanate particle. The TEM and SEM images showed average particles size of barium strontium titanate about 70-100 nm.

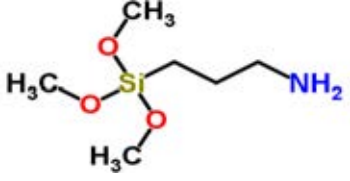
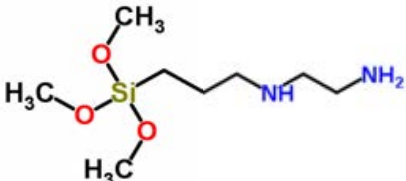
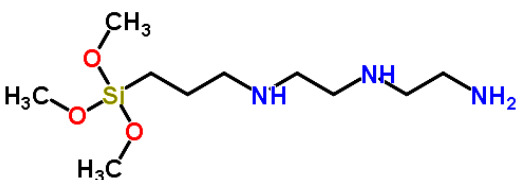
## **5.2 Surface modification of barium strontium titanate particles on composites**

The main problems of the polymer/ceramic composites are the poor dispersion of ceramic particles in the polymer matrix and the poor interaction between ceramic and polymer. The filler ( $\text{BaSrTiO}_3$ ) was then treated with a silane coupling agents in order to improve compatibility and dispersability with the polymer (polyimide) matrix.

General structures of the silane coupling agents are consisted of the different two functionalities, inorganic and organic group. The organic group reacts to form a chemical bond with polymer (polyimide). While, the inorganic group reacts with the surface of inorganic filler ( $\text{BaSrTiO}_3$  particles) to form a chemical bond. The interaction between polymer (polyimide) and ceramic filler ( $\text{BaSrTiO}_3$  particles) was thus enhanced by improved the interfacial adhesion strength and improved overall properties of the composites.

In this work, to study the effect of the surface modification on the properties of  $\text{BaSrTiO}_3$ /polyimide composites which the composites properties were compared between treated  $\text{BaSrTiO}_3$  and untreated  $\text{BaSrTiO}_3$  particles. The silane coupling agents were used in this research, as shown in Table 5.1

**Table 5.1** Type and structure of silane coupling agents

Type of silane coupling agents	Structure of silane coupling agents
3-aminopropyltrimethoxysilane (APTS)	
3-(2-aminoethylamino) Propyltrimethoxymethylsilane (AEPTS)	
3-[2-(2-aminoethylamino)ethylamino]propyl-trimethoxysilane (AEEPTS)	

### 5.2.1 Characterization of silane treated BaSrTiO<sub>3</sub> particles

#### 5.2.1.1 Functional groups of silane treated BaSrTiO<sub>3</sub> particles

The mechanism of silane coupling agent treatment on barium strontium titanate surface particles started with a silane coupling agent reaction with water by hydrolysis reaction to form a silanol group (Si-OH). After that the Si-OH group of silane coupling agent reacted with the hydroxyl groups on the surface of barium strontium titanate particles to form the Si-O-Si linkages, as shown in Figure 5.4.

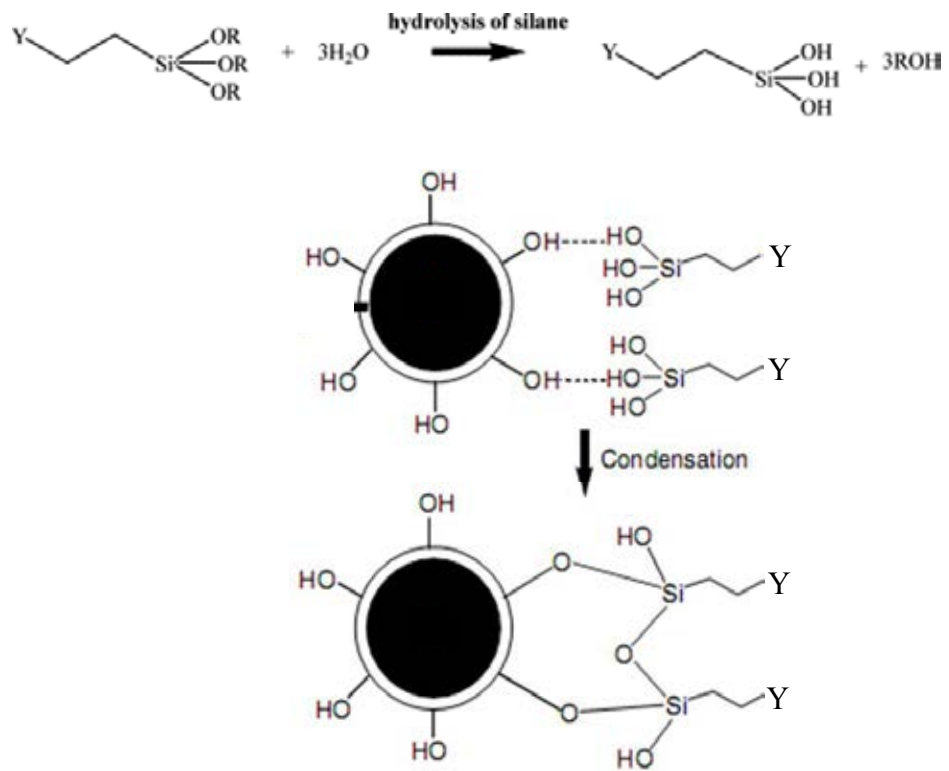


**Figure 5.4** The mechanism reaction of silane coupling agents on BaSrTiO<sub>3</sub> surface [36]



The surface chemistry of the barium strontium titanate particles were investigated by Fourier transformed infrared spectroscopy (FTIR), as shown in Figure 5.5 and Figure 5.6

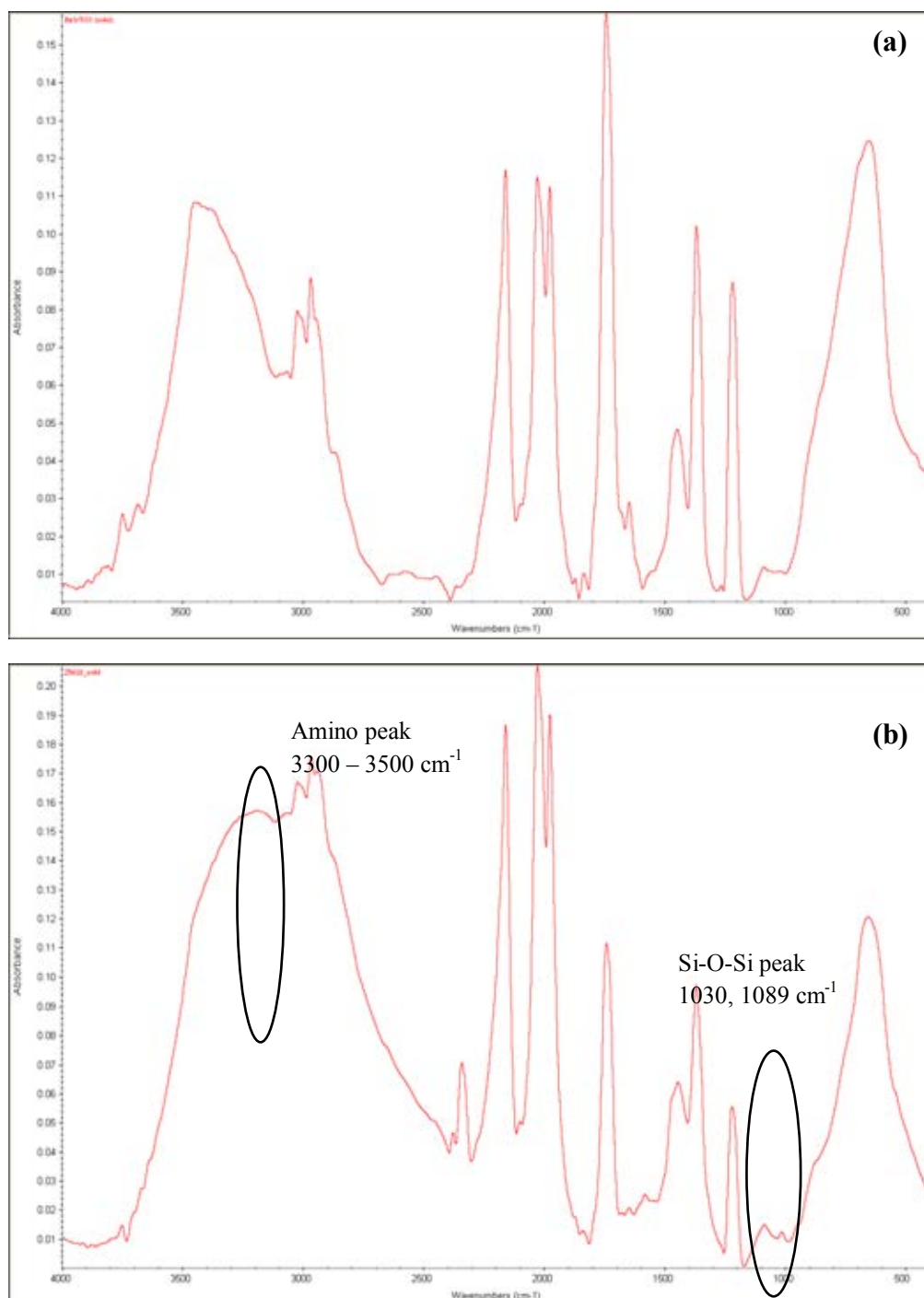


**Figure 5.5** FT-IR spectra of BaSrTiO<sub>3</sub> particles a) Untreated BaSrTiO<sub>3</sub>  
b) AEPTS silane treated BaSrTiO<sub>3</sub>

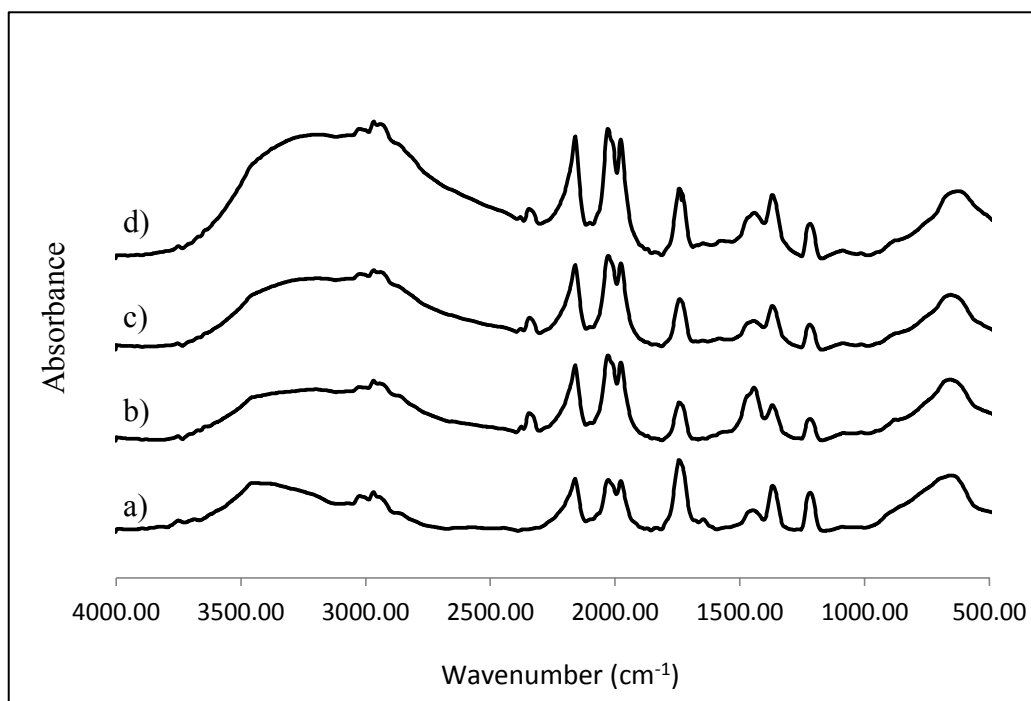


**Figure 5.6** FT-IR spectra of silane treated BaSrTiO<sub>3</sub> particles a) Untreated BaSrTiO<sub>3</sub> b) APTS silane treated BaSrTiO<sub>3</sub>, c) AEPTS silane treated BaSrTiO<sub>3</sub> and d) AEEPTS silane treated BaSrTiO<sub>3</sub>

In Figure 5.5 and 5.6, BaSrTiO<sub>3</sub> particles were modified by three types of the silane coupling agents which have different amino groups in chemical structure. The characteristic at wave number 3300-3500 cm<sup>-1</sup> and >3000 cm<sup>-1</sup> were observed in the FT-IR spectra corresponded with primary amino (NH<sub>2</sub>) and secondary amino (NH). Compared with the spectra of untreated BaSrTiO<sub>3</sub> particles and silane treated BaSrTiO<sub>3</sub> particles appeared a new absorption bands of Si-O-Si from the hydrolysis of silane coupling agents at wave number 1030 cm<sup>-1</sup> and 1089 cm<sup>-1</sup>. The organo functional groups of silane coupling agents were not easy to acquire due to the strong peak from adjacent other molecular vibrations. Moreover, these results confirmed that silane coupling agent could modify the BaSrTiO<sub>3</sub> surface successfully.

### 5.2.1.2 Morphology of untreated and silane treated BaSrTiO<sub>3</sub> particles

The morphology and particles size of BaSrTiO<sub>3</sub> particles were characterized by scanning electron microscopy (SEM) observation as shown in Figure 5.7 and 5.8.

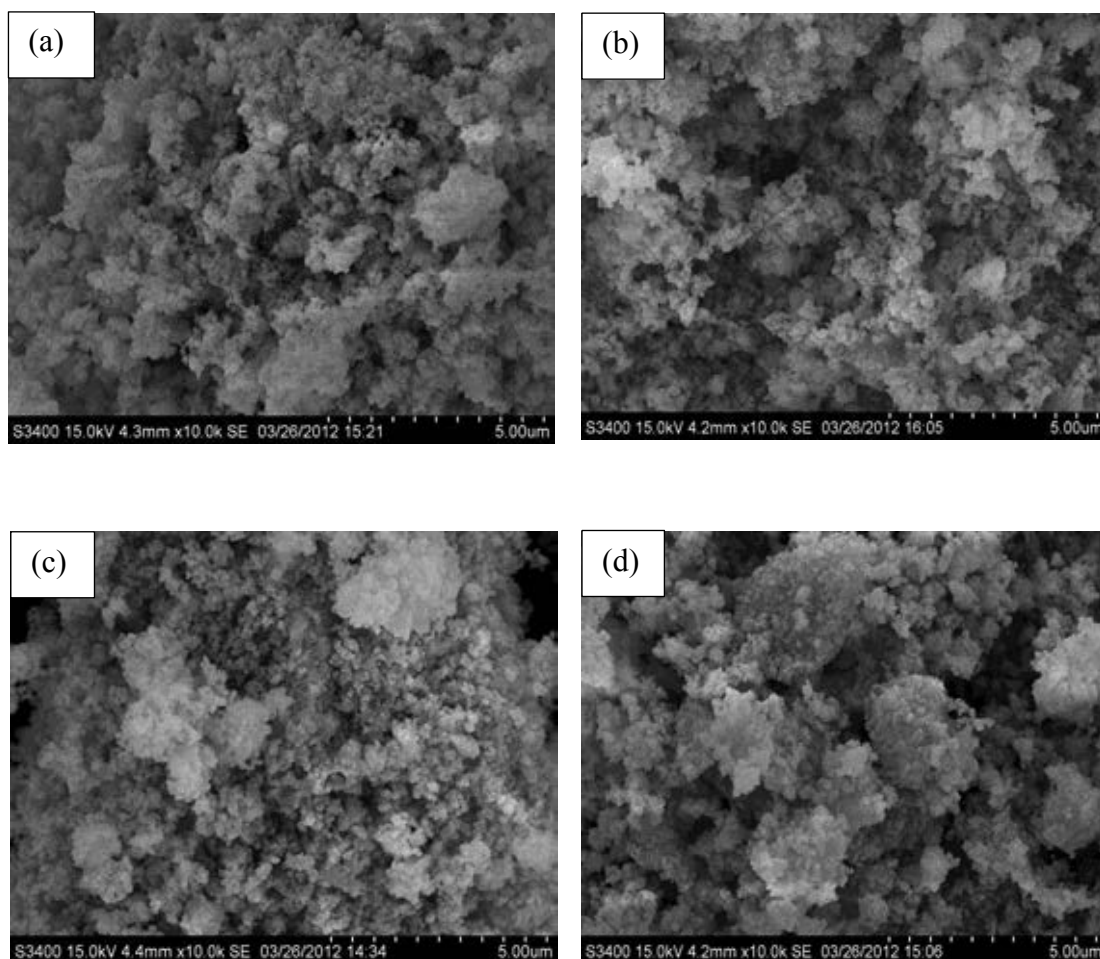


**Figure 5.7** Morphology of BaSrTiO<sub>3</sub> particles at  $\times 10k$  of magnification of SEM equipment a) Untreated BaSrTiO<sub>3</sub>, b) APTS silane treated BaSrTiO<sub>3</sub>, c) AEPTS silane treated BaSrTiO<sub>3</sub> and d) AEEPTS silane treated BaSrTiO<sub>3</sub>

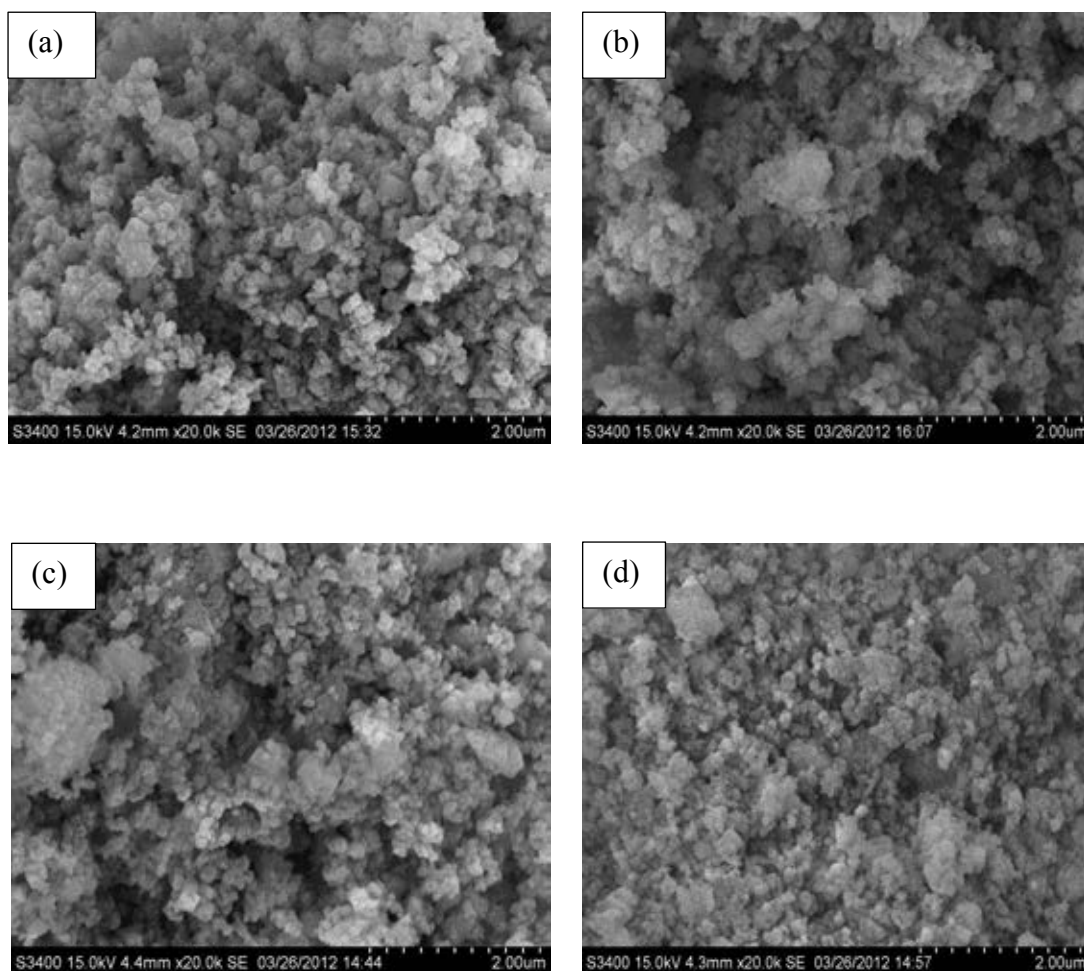


**Figure 5.8** Morphology of BaSrTiO<sub>3</sub> particles at  $\times 20k$  of magnification of SEM equipment a) Untreated BaSrTiO<sub>3</sub>, b) APTS silane treated BaSrTiO<sub>3</sub>, c) AEPTS silane treated BaSrTiO<sub>3</sub> and d) AEEPTS silane treated BaSrTiO<sub>3</sub>

In Figure 5.7 and 5.8, morphology of the untreated BaSrTiO<sub>3</sub> and the silane coupling agent were similar due to the thin monolayer of the silane coupling agents on surface of BaSrTiO<sub>3</sub> particles in order to prevent agglomeration of particles in the matrix polymer. The particles of BaSrTiO<sub>3</sub> were small and some particles were agglomerated to form large particles size. Average size of untreated BaSrTiO<sub>3</sub> and silane coupling agents treated BaSrTiO<sub>3</sub> particles were about 70-100 nm.

## 5.2.2 Characterization of silane treated BaSrTiO<sub>3</sub>/polyimide composite

### 5.2.2.1 Functional groups of silane treated BaSrTiO<sub>3</sub>/polyimide composite

In this section, the polyimides were prepared from Pyromellitic dianhydride (PMDA) and 4,4'-Oxydianiline (ODA) in N-methyl-2-pyrrolidinone (NMP) solvent to form poly(amic acid) by a two-step method. After that, the poly(amic acid) solution was then heat to remove solvent and subjected to thermal imidization to produce the polyimide. The structure of polyimide was characterized by Fourier transformed infrared spectroscopy (FTIR), as shown in Figure 5.9.

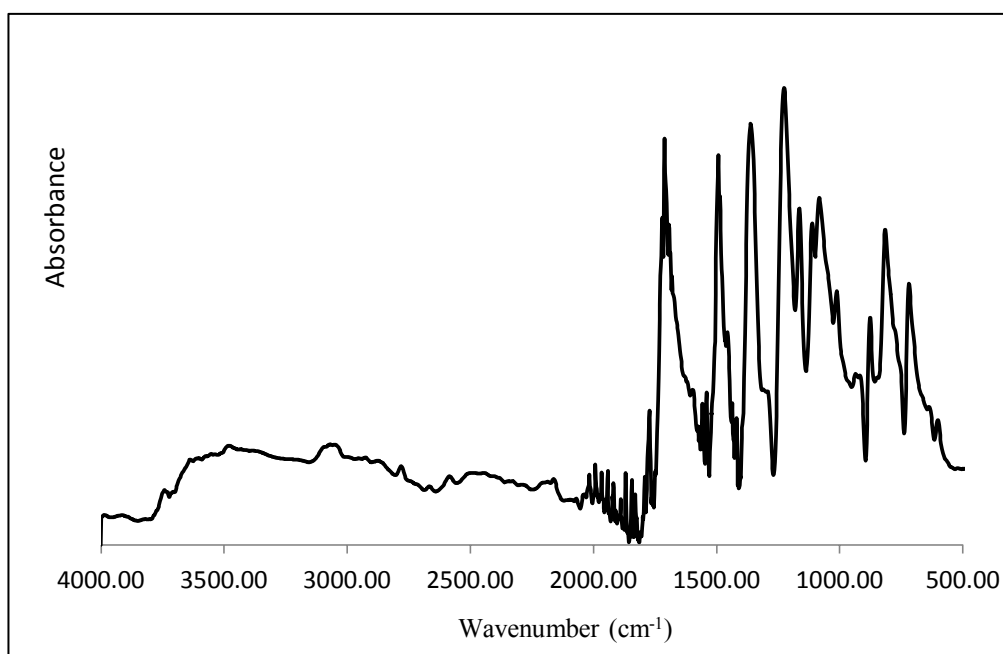


**Figure 5.9** FT-IR spectra of pure polyimide

The FT-IR spectra (Figure 5.9) showed that the imide absorption bands near 1780 cm<sup>-1</sup> (C=O asymmetrical stretching), 1720 cm<sup>-1</sup> (C=O stretching vibration) and 1380 cm<sup>-1</sup> (C–N stretching) behaved as common characteristic absorption peak of the imide group. [26,32] The peaks of poly(amic acid) were not appeared, indicated that the imidization reaction was completed.

The untreated and silane coupling agents treated of BaSrTiO<sub>3</sub> particles were dispersed in the matrix polyimide to form BaSrTiO<sub>3</sub>/polyimide composites. The

composite were characterized by Fourier transformed infrared spectroscopy (FTIR), as shown in Figure 5.10-5.13.

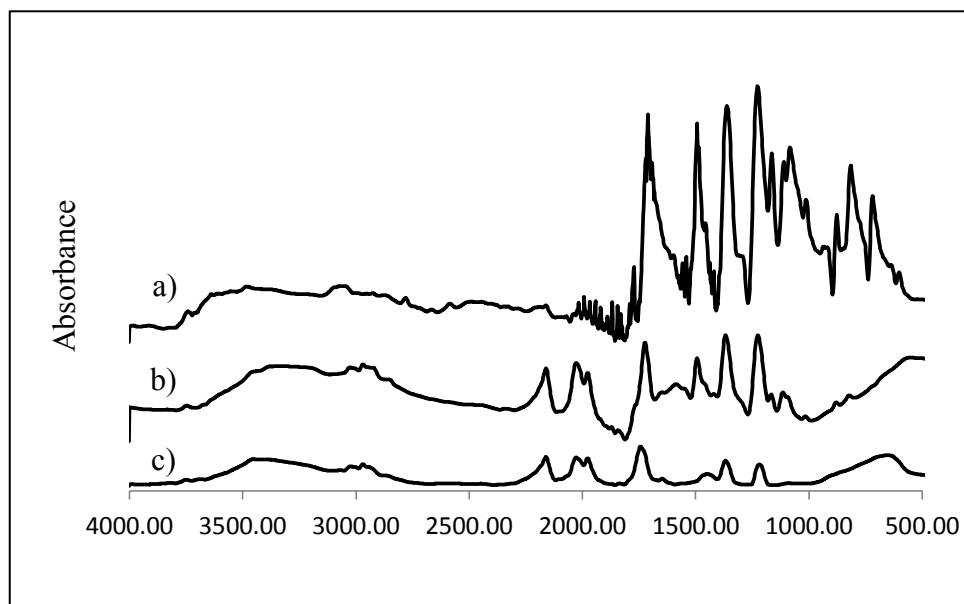


**Figure 5.10** FT-IR spectra of a) pure PI, b) untreated BaSrTiO<sub>3</sub>/PI composite and c) Untreated BaSrTiO<sub>3</sub> particles

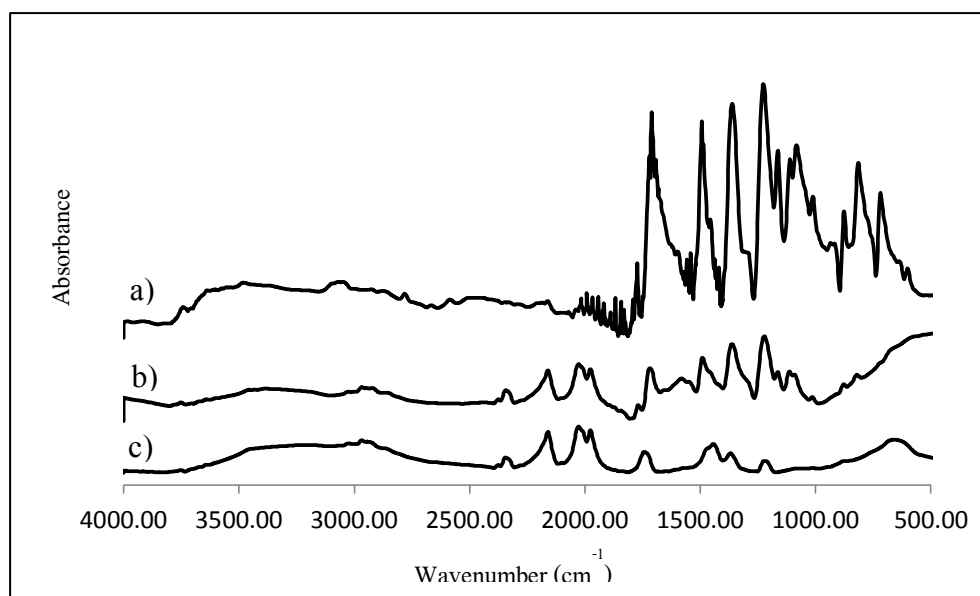


**Figure 5.11** FT-IR spectra of a) pure PI, b) APTS silane treated BaSrTiO<sub>3</sub>/PI composite and c) APTS silane treated BaSrTiO<sub>3</sub> particles

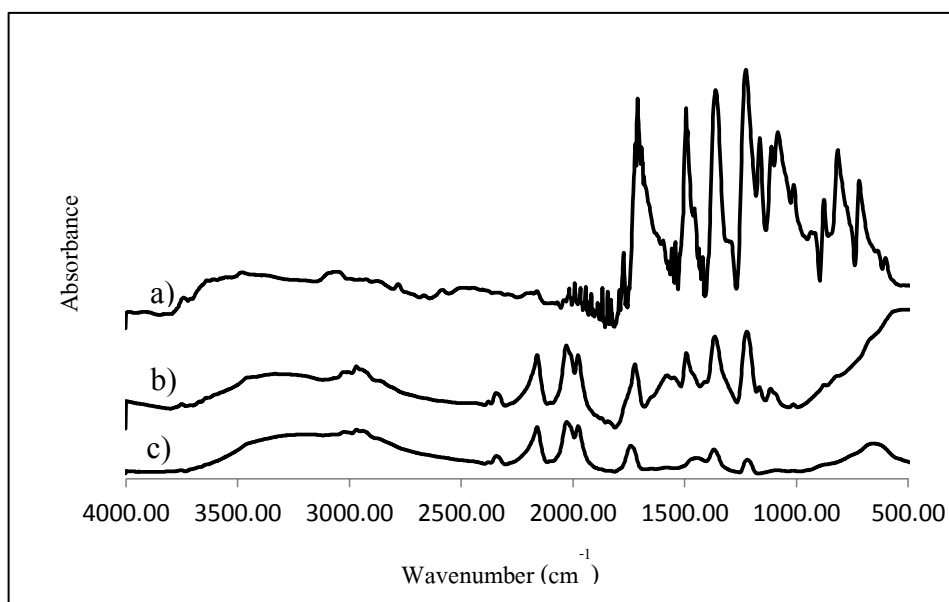


**Figure 5.12** FT-IR spectra of a) pure PI, b) AEPTS silane treated BaSrTiO<sub>3</sub>/PI composite and c) AEPTS silane treated BaSrTiO<sub>3</sub> particles

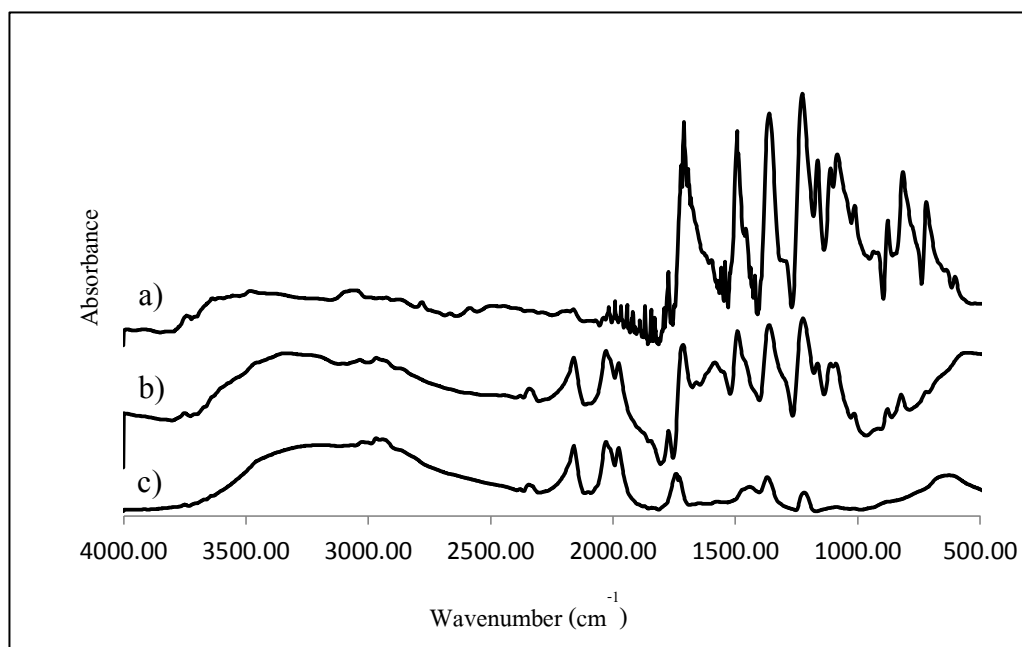


**Figure 5.13** FT-IR spectra of a) pure PI, b) AEEPTS silane treated BaSrTiO<sub>3</sub>/PI composite and c) AEEPTS silane treated BaSrTiO<sub>3</sub> particles

All BaSrTiO<sub>3</sub>/PI composite was investigated by FT-IR spectra as shown in Figure 5.10 – 5.13 to confirm the attachment of polyimide in composite. The spectra of untreated BaSrTiO<sub>3</sub> and three types of silane coupling agents treated BaSrTiO<sub>3</sub> with polyimide composite exhibited similar peaks as combination of nascent ingredient, that were the characteristic main peak at 1780 cm<sup>-1</sup> (C=O asymmetrical stretching), 1720 cm<sup>-1</sup> (stretching vibration) and 1380 cm<sup>-1</sup> (C–N stretching) as commonly the characteristic absorption peak of the imide group. In three types of silane treated BaSrTiO<sub>3</sub>/polyimide composites were exhibited peak of Si-O-Si vibration at 1000-1200 cm<sup>-1</sup> but It was difficult to identify because of the small content of silane coupling agents in the composites. [37] Confirmed from this FT-IR spectra, The polyimide and BaSrTiO<sub>3</sub> particles were completely developed to BaSrTiO<sub>3</sub>/polyimide composites.



### 5.2.2.2 Morphology of untreated and silane treated BaSrTiO<sub>3</sub>/polyimide composite

The morphology and dispersion of particles in polyimide were characterized by scanning electron microscopy (SEM) equipment, as show in Figure 5.14-5.16.

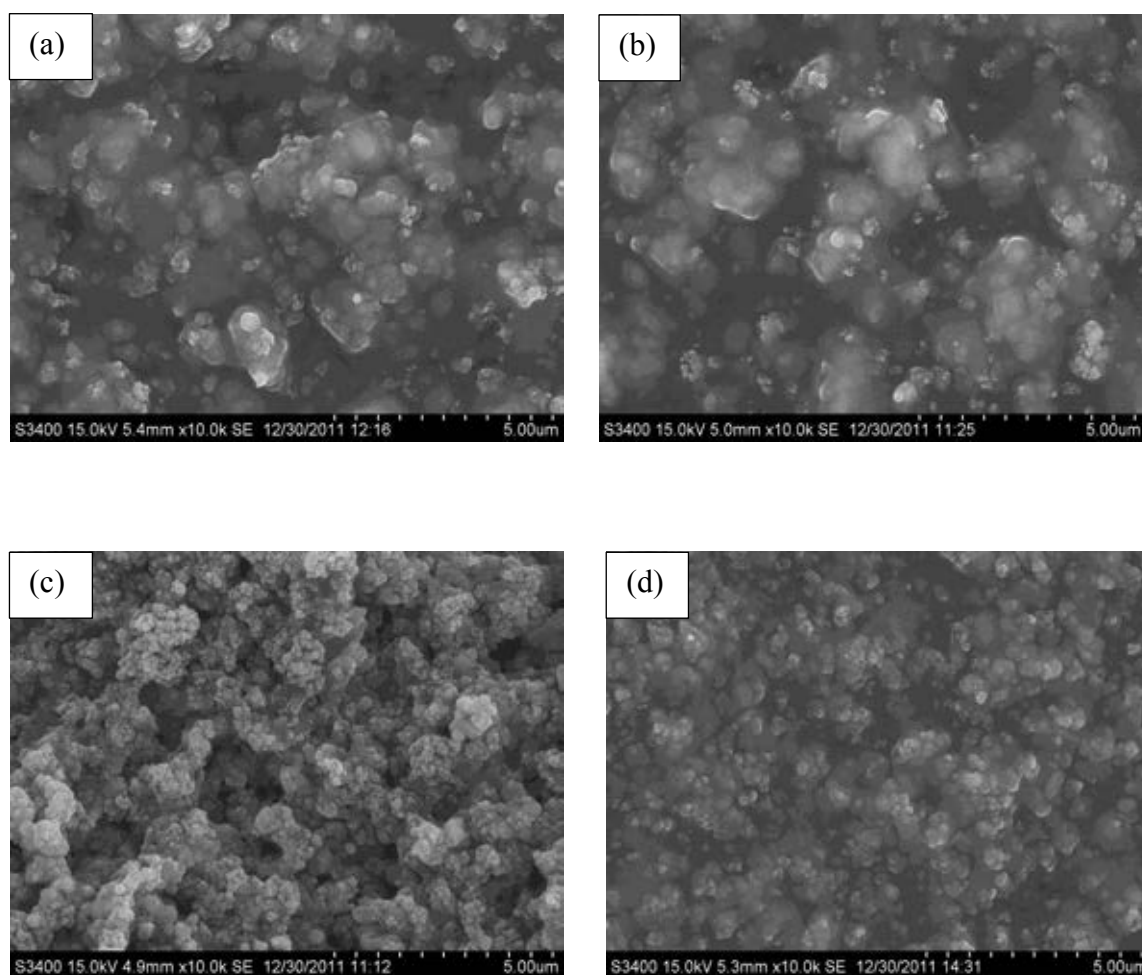


**Figure 5.14** Morphology of 70 wt% BaSrTiO<sub>3</sub>/polyimide composite at ×10k of magnification of SEM equipment a) untreated BaSrTiO<sub>3</sub>, b) APTS silane treated BaSrTiO<sub>3</sub>, c) AEPTS silane treated BaSrTiO<sub>3</sub> and d) AEEPTS silane treated BaSrTiO<sub>3</sub>

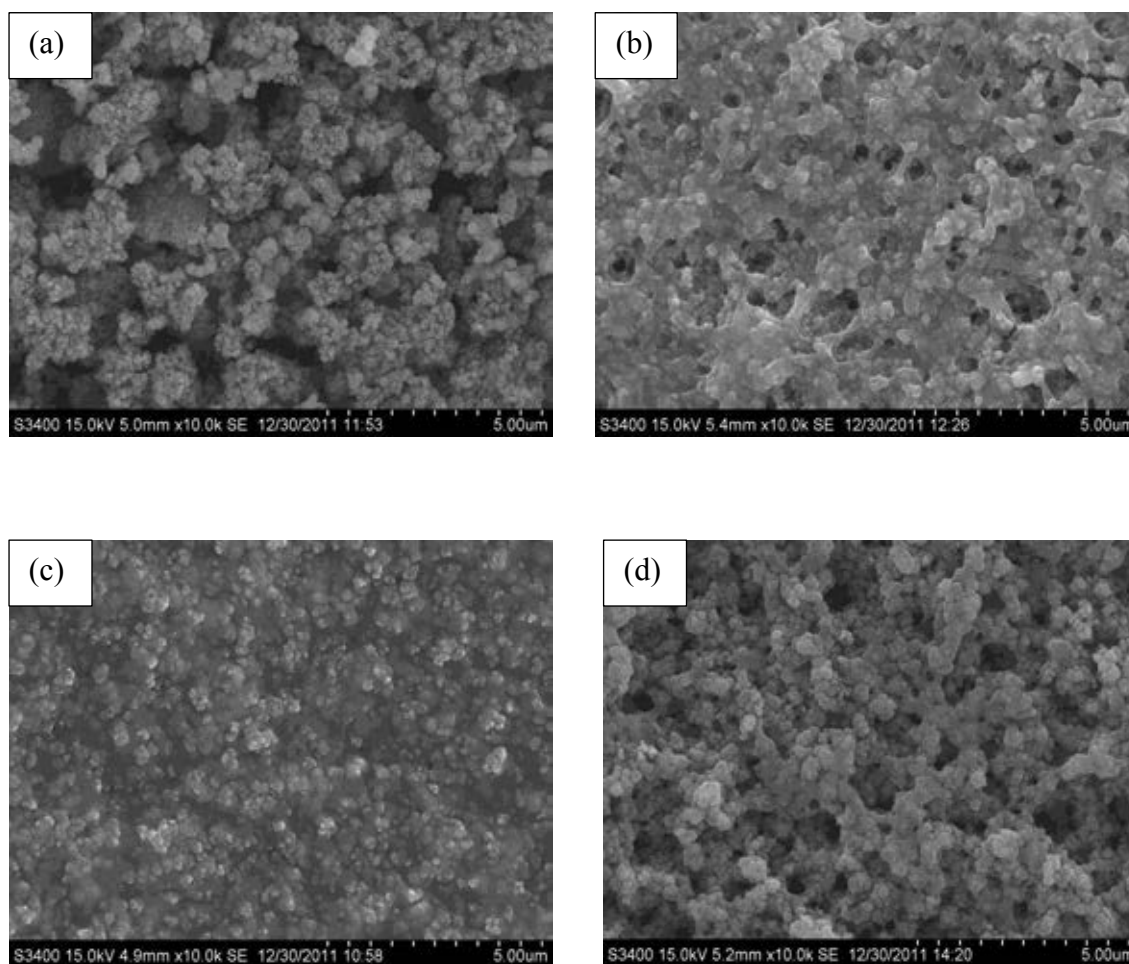


**Figure 5.15** Morphology of 90 wt% BaSrTiO<sub>3</sub>/polyimide composite at  $\times 10k$  of magnification of SEM equipment a) untreated BaSrTiO<sub>3</sub>, b) APTS silane treated BaSrTiO<sub>3</sub>, c) AEPTS silane treated BaSrTiO<sub>3</sub> and d) AEEPTS silane treated BaSrTiO<sub>3</sub>

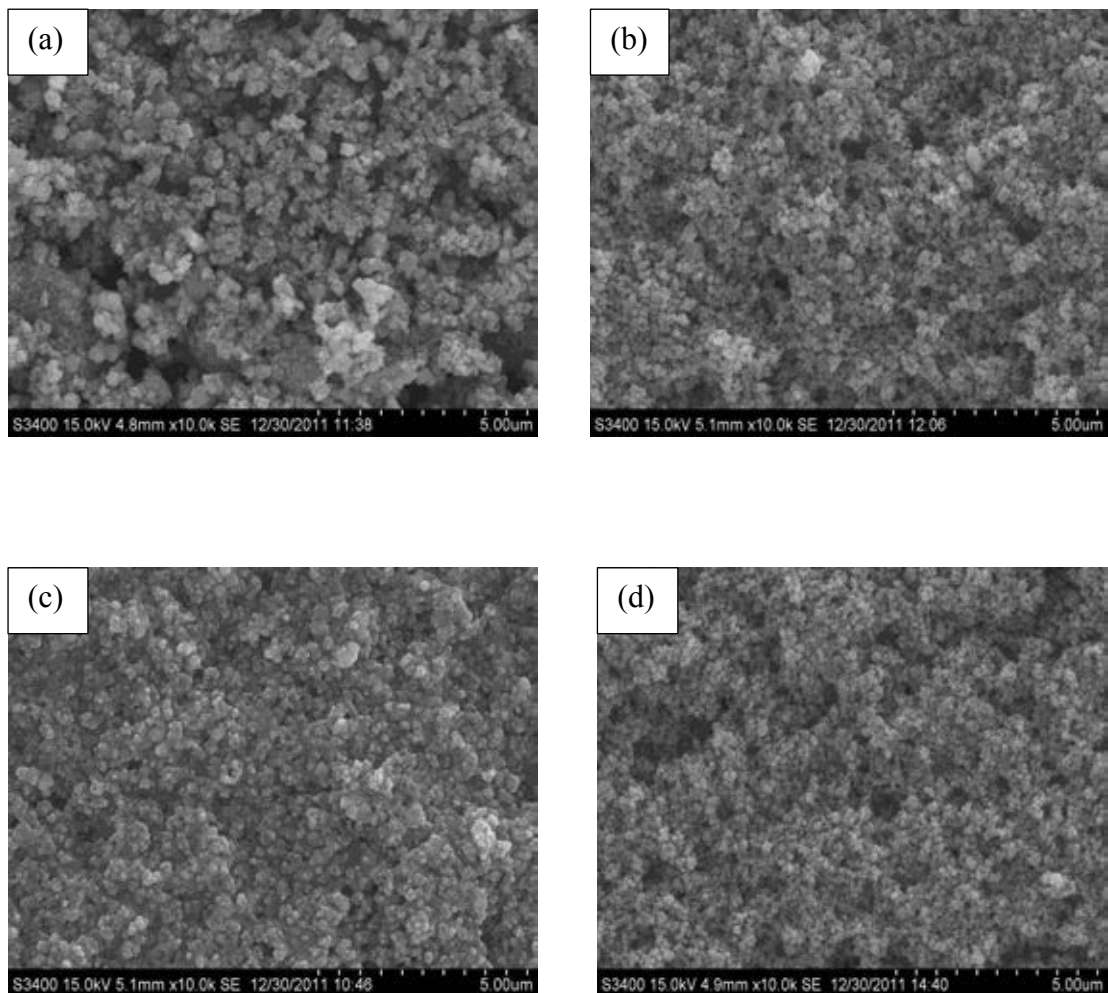


**Figure 5.16** Morphology of 95 wt% BaSrTiO<sub>3</sub>/polyimide composite at  $\times 10k$  of magnification of SEM equipment a) untreated BaSrTiO<sub>3</sub>, b) APTS silane treated BaSrTiO<sub>3</sub>, c) AEPTS silane treated BaSrTiO<sub>3</sub> and d) AEEPTS silane treated BaSrTiO<sub>3</sub>

In Figure 5.14-5.16, the SEM images revealed the dispersion and morphology of BaSrTiO<sub>3</sub> particles in the polyimide matrix at different weight content of BaSrTiO<sub>3</sub> particles and type of silane coupling agent. Compared between untreated and silane treated BaSrTiO<sub>3</sub> particle in polyimide, the silane treated BaSrTiO<sub>3</sub>/polyimide composite could reduce agglomeration of BaSrTiO<sub>3</sub> particles in polyimide matrix better than the untreated BaSrTiO<sub>3</sub>/polyimide composite at low concentration of BST, because a silane coupling agents could improve compatibility between BaSrTiO<sub>3</sub> filler and polyimide matrix. Moreover, the composites was increased the weight content of BaSrTiO<sub>3</sub> particles in polyimide matrix from 70 wt% to 97 wt% of BaSrTiO<sub>3</sub> particles while some particles of BaSrTiO<sub>3</sub> tended to form large particles are effect of agglomeration particles in polymer matrix was increased.

However, the usage of amino silane coupling agents treated BaSrTiO<sub>3</sub> particles can eliminate the agglomeration particles more than untreated BaSrTiO<sub>3</sub> particles as confirmed by SEM and improved other properties of the composite as discussed in next section.

### 5.2.2.3 Thermal properties of BaSrTiO<sub>3</sub>/polyimide composite

The thermal properties of pure polyimide, untreated BaSrTiO<sub>3</sub>/polyimide composite and three type silane treated BaSrTiO<sub>3</sub>/polyimide composite were investigated by Thermo gravimetric analysis (TGA) measurement, as shown in Figure 5.17.

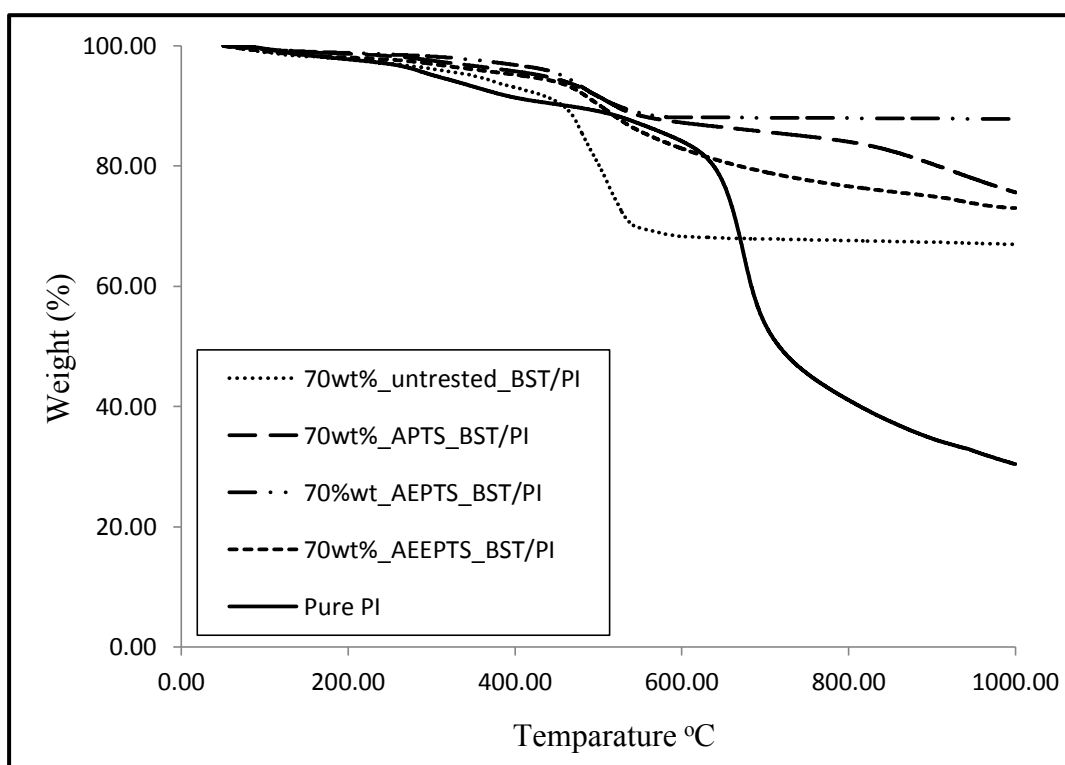


**Figure 5.17** Thermogram of 70wt% BaSrTiO<sub>3</sub>/polyimide composite and pure polyimide at N<sub>2</sub> atmosphere

Thermal properties from TGA analysis of pure polyimide, untreated BaSrTiO<sub>3</sub>/polyimide composite and composite at various type of the silane coupling agents are shown in Figure 5.17 and 5%weight loss temperatures and char yield at 1000°C are shown in Table 5.2. The char yield under nitrogen atmosphere implied remained of the inorganic group and interaction between silane, particles and polyimide.

**Table 5.2** Thermal stabilities of pure PI and BaSrTiO<sub>3</sub>/PI composite

Material	T <sub>d5%</sub> (C°) <sup>a</sup>	Char yield (%) <sup>b</sup>
Pure PI	303.5	30.39
70wt% of untreated BaSrTiO <sub>3</sub> /polyimide	349.83	66.96
70wt% of APTS treated BaSrTiO <sub>3</sub> /polyimide	432.5	75.6
70wt% of AEPTS treated BaSrTiO <sub>3</sub> /polyimide	457.33	87.78
70wt% of AEEPTS treated BaSrTiO <sub>3</sub> /polyimide	408.66	72.99

<sup>a</sup> 5% Mass loss temperature under nitrogen

<sup>b</sup> Char yield at 1000 °C under nitrogen

The pure polyimide have T<sub>5%</sub> and char yield at 303.5 °C and 30.39%, respectively. The pure polyimide showed lower thermal stabilities than the composite contain filler because the presence of BaSrTiO<sub>3</sub> restrained the movement of polyimide main chain and limited the segmental movements in the polyimide matrix. [37] However, the pure polyimide is not showed char yield equal to zero due to the highly stable carbon structure from inorganic group.

The AEPTS silane treated BaSrTiO<sub>3</sub>/polyimide composite showed highest thermal stabilities of T<sub>d5%</sub> at 457.33 °C and 87.78% char yield. Compared with untreated BaSrTiO<sub>3</sub>/polyimide composite showed lower thermal stabilities than the AEPTS silane treated BaSrTiO<sub>3</sub>/polyimide composite due to the amino groups of silane coupling agents were coordinated between polymer and ceramic filler, resulting in the difficulty to thermally decompose the covalent bonds of crosslinking network. Moreover, the APTS silane treated BaSrTiO<sub>3</sub>/polyimide composite showed lower thermal stability than the AEPTS silane treated BaSrTiO<sub>3</sub>/polyimide composite because the APTS silane treated BaSrTiO<sub>3</sub>/polyimide composite has lower amine

group than the AEPTS silane treated composite so the interaction and crosslinking network is lower than the AEPTS silane treated composite. However, the AEEPTS silane treated composite showed lowest thermal stability among all silane composite because the small amount of polyimide (30%w) is not enough to totally react with three amines of AEEPTS silane coupling agent. Moreover, the remained of untreated composite at 1000°C was below 70%, the amount of BaSrTiO<sub>3</sub> particles in composite because of the inaccurate of the weight process in preparation the small amount of BaSrTiO<sub>3</sub> composite (polyimide char yield was 0.09% at 70% BaSrTiO<sub>3</sub>).

#### 5.2.2.4 Electrical properties of BaSrTiO<sub>3</sub>/polyimide composite

The dielectric constants can be determined as the equation below,

$$k = Cd/AK_0$$

C is the measured capacitance at any frequency

d is thickness of sample

A is area of sample

K<sub>0</sub> is free permittivity = 8.854 pF

The capacitances were measured via electronic circuit and used for calculation of the dielectric constant of composite. The dielectric losses were also investigated by LCR meter. The dielectric values of BaSrTiO<sub>3</sub>/polyimide composites at various type of silane coupling agents, frequency, filler content and different type of particles were summarized in Appendix E. The results show that the dielectric constants improved with increase in filler content at low frequency.

Figure 5.18 shows the dielectric constants and dielectric loss of composite as a function of the type of silane coupling agent with the increase of filler content at 100 kHz. The dielectric constant of all composite increased with the increase of filler content because the electrons traveled pass the composite easier in the more BaSrTiO<sub>3</sub> particles environment and less insulated properties of polyimide as the ratio BaSrTiO<sub>3</sub> was increased. At 99 wt% loading of BaSrTiO<sub>3</sub>, the dielectric constants were

decreased because more voids or pores were formed in composites to accommodate excess BaSrTiO<sub>3</sub> particles, over the maximum packing density. Voids or pores would behave as low dielectric resistance in composite, so the total dielectric was lower.

The dielectric constant of untreated BaSrTiO<sub>3</sub>/polyimide composite exhibited higher value than the dielectric constant of composite, modified by three type silane coupling agent due to the electrical insulation on surface of BaSrTiO<sub>3</sub> as induced by silane coupling agent. The insulation surface induced difficulty for the charge carriers to pass through the material. The untreated BaSrTiO<sub>3</sub>/polyimide composite exhibited the highest dielectric constant and dielectric loss at 97wt% loading of BaSrTiO<sub>3</sub> particles about 158 and 0.34, respectively at 100 kHz. The dielectric loss is the result from the heating effect on the dielectric material between the conductors in alternating current. The dielectric loss of composite increase with filler content that because of the attraction among molecular of dielectric materials.

Among three type of silane coupling agents, the APTS silane treated BaSrTiO<sub>3</sub>/polyimide composite showed the higher dielectric constants more than the AEPTS and AEEPTS silane treated BaSrTiO<sub>3</sub>/polyimide composite. However, the AEEPTS silane treated BaSrTiO<sub>3</sub>/polyimide composite has the lowest dielectric loss, the required properties for embedded capacitor.



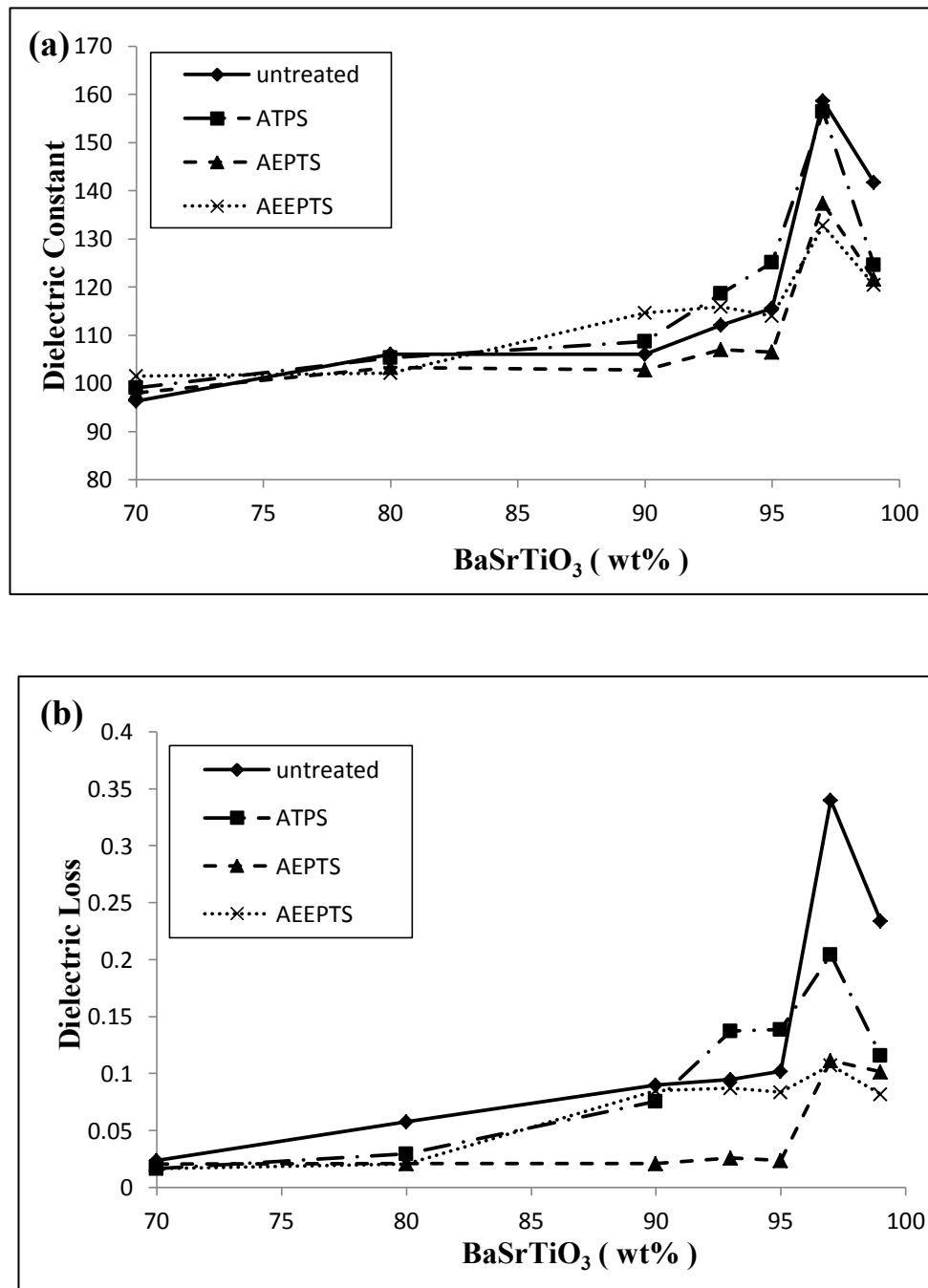


**Figure 5.18** Dielectric properties between untreated and various silane treated BaSrTiO<sub>3</sub>/polyimide composite at 100 kHz a) dielectric constant and b) dielectric loss

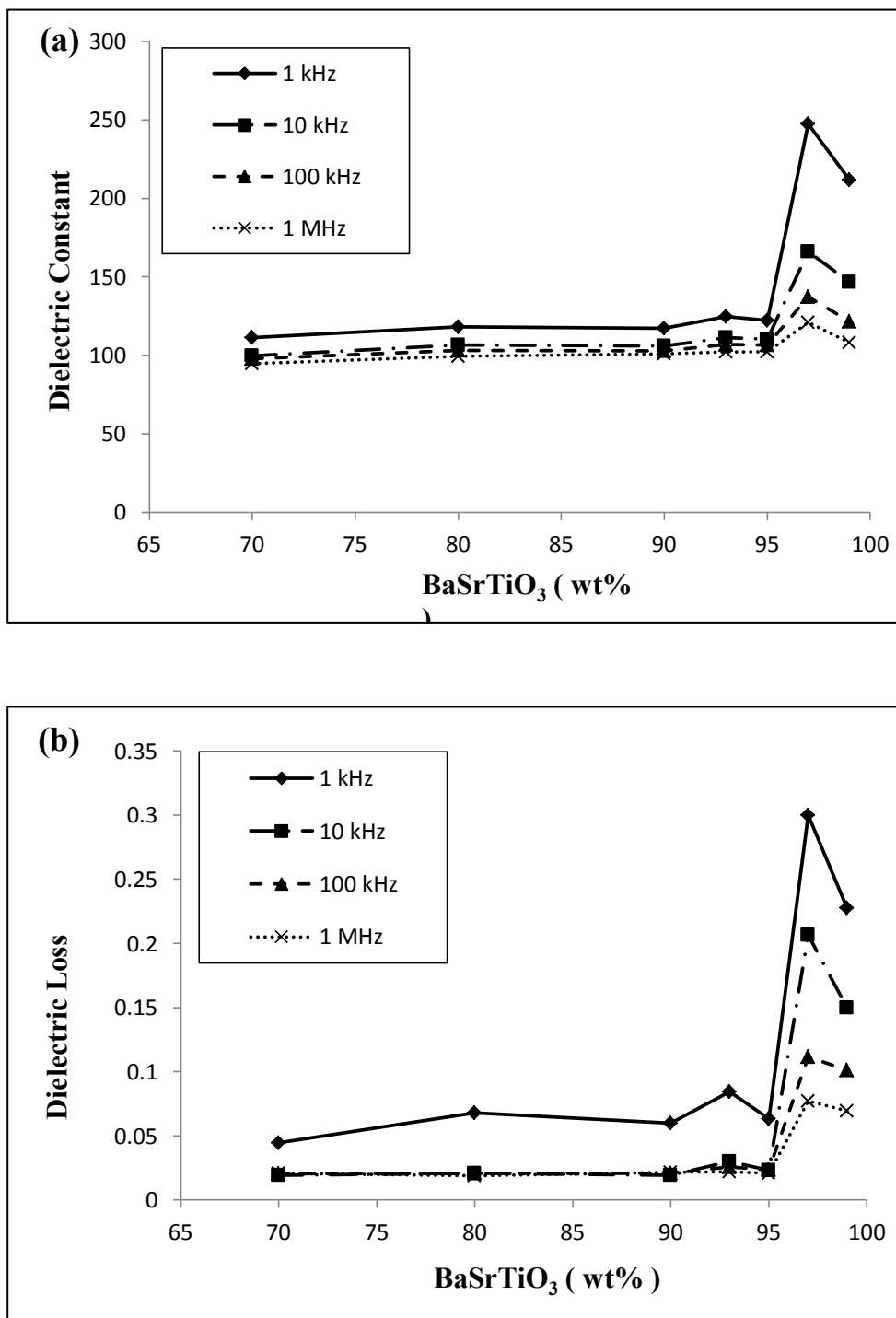
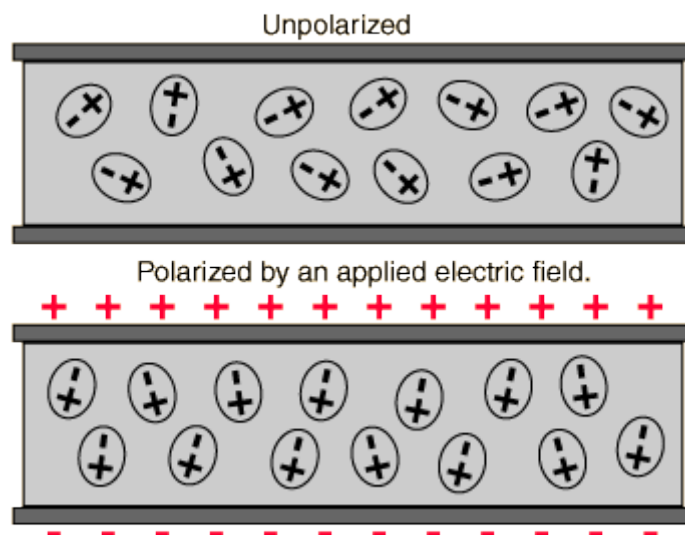


**Figure 5.19** Dielectric properties various frequency of AEPTS silane treated BaSrTiO<sub>3</sub>/polyimide composite a) dielectric constant and b) dielectric loss

The effect of frequency on dielectric properties of APTS silane treated BaSrTiO<sub>3</sub>/polyimide composite was shown in Figure 5.19. The dielectric constant and dielectric loss of composites decreased with increasing frequency of source due to polarization effect of dielectric material with electrical field. The material, contained polar molecules, would generally be in random orientations when no electric field is applied. An applied electric field would polarize the material by orienting the dipole moments of polar molecules. [38] At high frequency, the atoms of materials were decreased vibration, related to dielectric constant of composites. The comparison between polarization and non-polarization effect of material were showed in Figure 5.20.



(Ref: <http://hyperphysics.phy-astr.gsu.edu/hbase/electric/dielec.html>)

**Figure 5.20** Polarization of dipole material [38]

### 5.3 Hybridization of the SrTiO<sub>3</sub>/BaTiO<sub>3</sub>/polyimide composite

The different size of ceramics particles can cause positive effect on properties of the ceramic/polymer composite and was interesting because the different size particles can improve electric properties such as dielectric constant of composite. due to this effect, the dielectric constant can be increased because of the higher powder packing density and the success of reduction of void between these particles form insertion of small size particle to the grab of big size particles.

Strontium titanate (SrTiO<sub>3</sub>) particles were chosen to mix with BaSrTiO<sub>3</sub> particles in order to improve electrical properties because it has low dielectric loss and stable electrical properties at high temperature.

In this work, the BaSrTiO<sub>3</sub> and SrTiO<sub>3</sub> were exhibited average particles size about 70-100 nm and less than 5 μm respectively. The both were selected as a filler of the SrTiO<sub>3</sub>/BaSrTiO<sub>3</sub>/polyimide hybrid composite in order to investigate the effect of different particles size on dielectric constant and dielectric loss. In the past section, the APTS silane coupling agent showed higher dielectric properties of composite than the other silane coupling agent, so the APTS silane coupling agent was chosen to treated BaSrTiO<sub>3</sub> and SrTiO<sub>3</sub> particles in order to improve dispersion of particles in polyimide matrix. The morphology and average particles sizes were investigated by scanning electron microscopy (SEM), as shown in Figure 5.21.

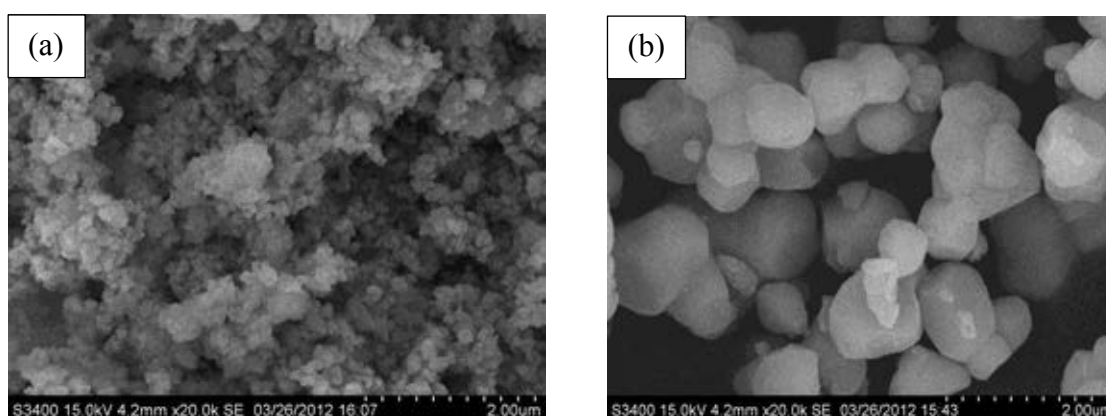


**Figure 5.21** Morphology of APTS silane treated filler a) BaSrTiO<sub>3</sub> and b) SrTiO<sub>3</sub>

### 5.3.1 Morphology of the SrTiO<sub>3</sub>/BaSrTiO<sub>3</sub>/polyimide hybrid composite

Scanning electron microscopy (SEM) is the useful equipment for analyzing morphology and dispersion of particles in the polymer matrix. The morphology of the SrTiO<sub>3</sub>/BaSrTiO<sub>3</sub>/polyimide hybrid composites can be shown in Figure 5.22 and 5.23.

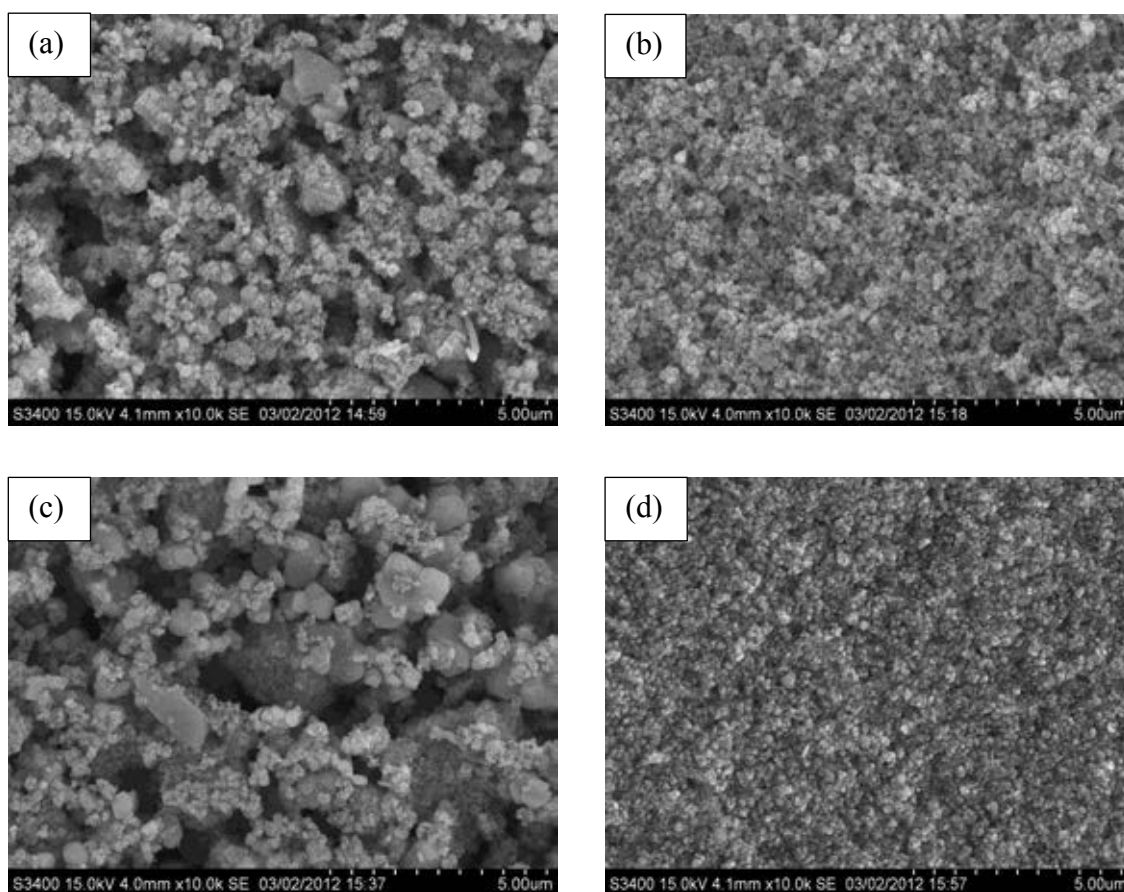


**Figure 5.22** Morphology of APTS silane treated SrTiO<sub>3</sub>/BaSrTiO<sub>3</sub>/polyimide hybrid composite at 97%wt of overall filler contents a) 5%wt SrTiO<sub>3</sub>, b) 10%wt SrTiO<sub>3</sub> c) 25%wt SrTiO<sub>3</sub> and a) 75%wt SrTiO<sub>3</sub>

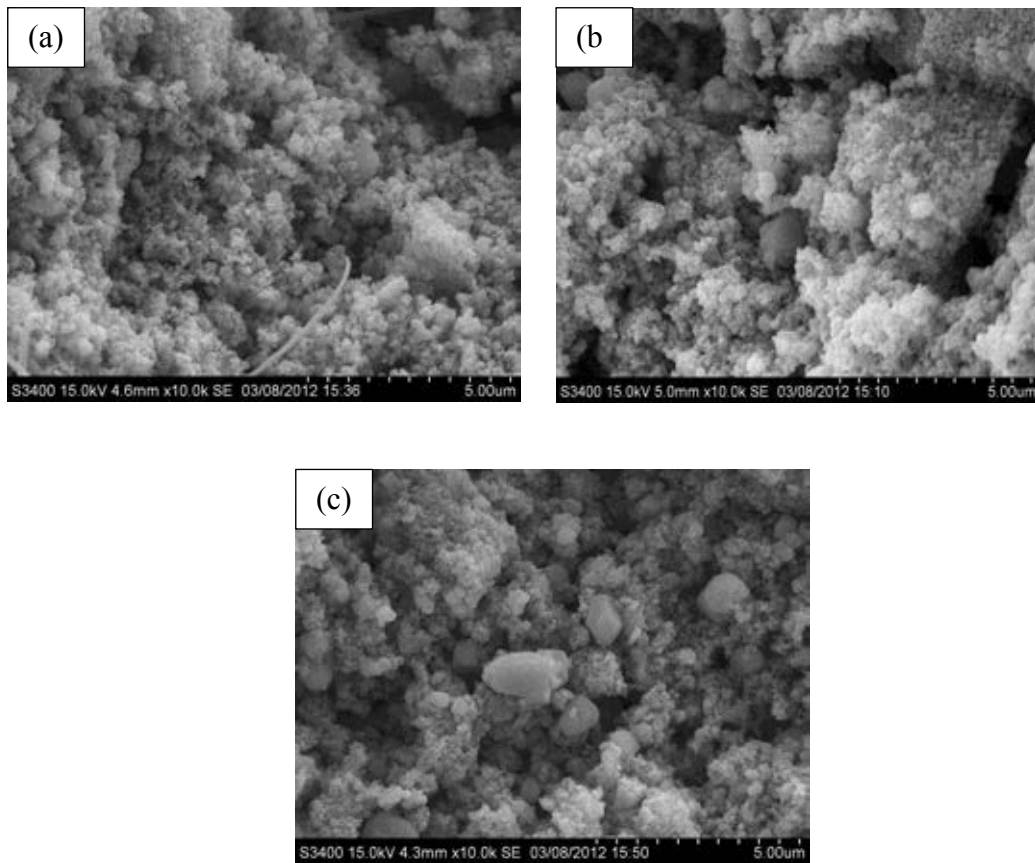


**Figure 5.23** Side section morphology of APTS silane treated SrTiO<sub>3</sub>/BaSrTiO<sub>3</sub>/polyimide hybrid composite at 97%wt of overall filler contents  
 a) 5%wt SrTiO<sub>3</sub>, b) 10%wt SrTiO<sub>3</sub>, and c) 15%wt SrTiO<sub>3</sub>

The SEM micrographs, illustrated in Figure 5.22 and 5.23, show the distribution of SrTiO<sub>3</sub> and BaSrTiO<sub>3</sub> particles in polyimide matrix at various composite loading of SrTiO<sub>3</sub> and BaSrTiO<sub>3</sub> in 97wt% total ceramics. Compared with the homogeneous particles size, the different particles size system, hybrid particle size system, could reduce void and improve packing density of the composite because a small particle size enhanced more packing with a large particle size. So, by this reason, it can cause positive effect on dielectric properties of the SrTiO<sub>3</sub>/BaSrTiO<sub>3</sub>/polyimide hybrid composite, as described in the next section.

### 5.3.2 Electrical properties of the SrTiO<sub>3</sub>/BaSrTiO<sub>3</sub>/polyimide hybrid composite

The electrical properties of the SrTiO<sub>3</sub>/BaSrTiO<sub>3</sub>/polyimide hybrid composites were investigated by LCR meter as shown in Figure 5.24.

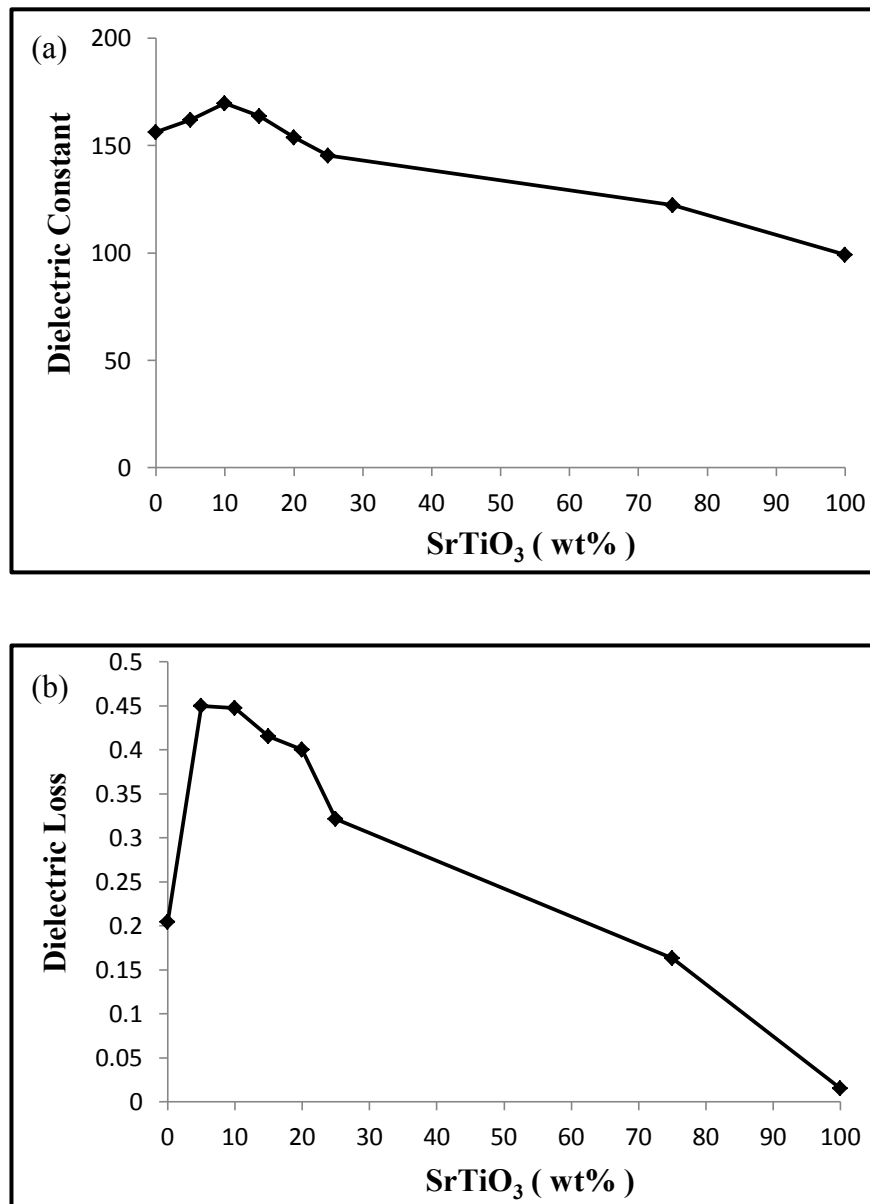


**Figure 5.24** Dielectric properties of APTS silane treated SrTiO<sub>3</sub>/BaSrTiO<sub>3</sub>/polyimide hybrid composite at 97%wt of overall filler contents at 100 kHz a) dielectric constant and b) dielectric loss

Figure 5.24 shows the effect of different particles size on the dielectric properties of the APTS silane treated SrTiO<sub>3</sub>/BaSrTiO<sub>3</sub>/polyimide hybrid composite at 97%wt of overall filler contents at 100 kHz. The hybrid particle size system showed higher dielectric constant than the same particles size system at the same frequency because, in this system, the voids and porosity tended to decrease. The dielectric constant was increased because the pores behaved as air, natural electrical insulation, in the mixture. The dielectric constant of composite increase to the maximum when the mass loading of SrTiO<sub>3</sub> increased up to 10 wt% with dielectric constant and dielectric loss about 169.73 and 0.447 respectively, at 100 kHz. When the SrTiO<sub>3</sub> particles were increased further, the dielectric constant decreased due to the unbalance in packing of the composite because of the increase in void and pore in composite from incorporation of large particles size of SrTiO<sub>3</sub>.



## CHAPTER VI

### CONCLUSIONS & RECOMMENDATIONS

#### 6.1 Conclusions

In this research, the synthesis method of barium strontium titanate( $\text{BaSrTiO}_3$ ), the preparation of surface modification by using the difference types of silane coupling agents and the properties of  $\text{BaSrTiO}_3$ /polyimide composite consisted of morphology, dielectric constant and thermal stability were investigated. The conclusions of this research can be summarized as follows;

1. The agglomerations of particles were increased at high filler content in composites regardless of the silane added.
2. The surface modification by three types of silane coupling agent could improve dispersion of particles in composite at low filler content.
3. The  $T_{d5\%}$  of  $\text{BaSrTiO}_3$ /polyimide exhibited higher values than the pure polyimide due to the presence of  $\text{BaSrTiO}_3$  which restrained the movement of polyimide main chains and limited the segments movements in the polyimide matrix.
4. The surface treatment of composite showed higher  $T_{d5\%}$  and % char yield than the untreated  $\text{BaSrTiO}_3$ /polyimide composite because the amino groups of silane coupling agents were coordinated between polymer and ceramic filler, resulted in the difficulty to thermally decompose the covalent bonds of crosslinking network.
5. The dielectric constant and dielectric loss of all composite increased with the increasing filler content and decreased with increasing frequency of source due to polarization effect of dielectric material.

6. The unimodal composite showed maximum dielectric constant of the untreated BaSrTiO<sub>3</sub>/polyimide composites at 97% weight content of filler about 158 at 100 kHz.
7. The silane coupling agents treated particles of composite showed lower dielectric constant and dielectric loss than the untreated BaSrTiO<sub>3</sub>/polyimide composite. However, the silane coupling agents are very important for composite due to it can reduce dielectric loss of composite that contributed to main requirement factor for embedded capacitor.
8. The packing density of composites was increased because of the effect of different ceramic particle size due to the reduction in void and pore in composite, so the dielectric constants were improved. The bimodal composite showed highest dielectric constant about 169 at 100 kHz (10 wt% of SrTiO<sub>3</sub>) with APTS silane treated filler.
9. The optimum conditions for embedded capacitor are 95 wt% of AEPTS silane treated BaSrTiO<sub>3</sub>/polyimide composites because it gave the highest dielectric constant (107 at 100 kHz) with dielectric loss of 0.024. However, if the economics in using the valuable filler was considered, the 70wt% of AEPTS silane treated BaSrTiO<sub>3</sub>/polyimide composites that give dielectric constant 98 at 100 kHz with dielectric loss of 0.021 might be more appropriated with 30% saving the filler.

## 6.2 Recommendations

6.2.1 Study the effect of different particle size of same type ceramic filler, BST if possible.

6.2.2 The other chemical structures of coupling agents should be investigated to find the suitable coupling agents for the BST material such as titanate coupling agents.

## REFERENCES

- [1] Naga, G. D.; Eung S. K.; and Burtrand I. L. The synthesis and dielectric study of BaTiO<sub>3</sub>/polyimide nanocomposite films. Journal of Microelectronic Engineering 82 (2005): 71–83.
- [2] Sung, D. C.; Joo, Y. L.; Jin, G. H.; and Kyung, W. P. Study on epoxy/BaTiO<sub>3</sub> composite embedded capacitor films (ECFs) for organic substrate applications. Journal of Materials Science and Engineering B 110 (2004): 233–239.
- [3] Seung, H. C.; Il, D. K.; Jae, M. H.; Ki, H. P.; and Seong, G.O. Effect of the dispersibility of BaTiO<sub>3</sub> nanoparticles in BaTiO<sub>3</sub>/polyimide composites on the dielectric properties Journal of Materials Letters 61 (2007): 2478 – 2481.
- [4] Shu, H. X.; Bao, K. Z.; Zhi, K. X.; and You, Y. X. Preparation and properties of polyimide/LTNO composite films with high dielectric constant Journal of Materials Letters 59 (2005): 2403 – 2407.
- [5] Kobayashi, Y.; Kosuge, A.; and Konno, M. Fabrication of high concentration barium titanate/polyvinylpyrrolidone nano-composite thin films and their dielectric properties. Journal of Applied Surface Science 255 (2008): 2723–2729.
- [6] Kholam, Y. B.; Deshpande, S. B.; Potdar H. S.; Bhoraskar S. V.; Sainkar S. R.; and Date S. K. Simple oxalate precursor route for the preparation of barium–strontium titanate: Ba<sub>1-x</sub>Sr<sub>x</sub>TiO<sub>3</sub> powders. Journal of Materials Characterization 54 (2005): 63-74.
- [7] Hari, S. N. Handbook of Thin Film Material. Academic Press: San Diego, 2002.
- [8] Sroog, C. E. Polyimides. Journal of Polymer science 16 (1991): 561-694.

- [9] Wang, F. J.; Li, W.; Xue, M. S.; Yao J. P.; and Lu, J. S. BaTiO<sub>3</sub> – polyethersulfone nanocomposites with high dielectric constant and excellent thermal stability. Journal of Composites Part B. 42 (2011): 87–91.
- [10] Debra, L. D. Synthesis and characterization of thermosetting polyimide oligomers for microelectronics packaging. Doctoral dissertation, Faculty of Chemistry, Virginia Polytechnic Institute, 2000.
- [11] Wikipedia. Polyimide [online]. 2010. Available from: <http://en.wikipedia.org/wiki/Polyimide.html> [2012, January 10]
- [12] Thomas, R.; Richard G.; and Beth, B. Characterization of Barium Strontium Titanate Films Using XRD. Journal of Applied Polymer 34 (1995): 50-77.
- [13] Tiggelman, M. P.J. Thin film barium strontium titanate capacitors for tunable FR front-end applications. Doctoral dissertation, Faculty of Engineering, University of Twente, Netherlands, 2009.
- [14] Bud, N. Thin Film Barium Strontium Titanate (BST) for a New Class of Tunable RF Components [Online]. 2004. Available from: <http://www.microwavejournal.com/articles/1673-thin-film-barium-strontium-titanate-bst-for-a-new-class-of-tunable-rf-components.html> [2012, January 14]
- [15] Berbecaru, C.; Alexandru, H. V.; Porosnicu, C.; Velea, A.; Ioachim, A.; Nedelcu, L.; and Tonsan, M. Ceramic materials Ba(1-x)SrxTiO<sub>3</sub> for electronics - Synthesis and characterization. Thin Solid Films 516 (2008): 8210-8214.
- [16] Bo, H.; Yao, X.; Dong, W.; and Yuhan, S. Preparation and characterization of single-crystalline barium strontium titanate nanocubes via solvothermal method. Journal of Powder Technology 170 (2006): 26 – 30

- [17] Mao, C.; Dong, X.; and Zeng, X. Synthesis and characterization of nanocrystalline barium strontium titanate powders prepared by citrate precursormethod. Journal of Materials Letters 61 (2007): 1633-1636.
- [18] Aegerter, M. A.; Almeida, R.; Soutar, A.; Tadanaga, K.; Yang, H.; and Watanabe, T. Coatings made by sol-gel chemical nanotechnology. Journal of Sol-Gel Science Technology 47 (2008): 203-236.
- [19] ChewFeng, K.; and Wein, D. Y. Preparation and electrical characterisation of strontium titanate ceramic from titanyl acylate precursor in strong alkaline solution. Ceramic International 22 (1996): 57-66.
- [20] Azom. Strontium titanate properties [online]. 2004. Available from: <http://www.azom.com/article.aspx?ArticleID=2362.html> [2012, January 16]
- [21] Reade Co., Ltd. Strontium titanate powder [online]. 2008. Available from: <http://www.reade.com/home/748.html> [2012, January 15]
- [22] Plueddemann. Silane coupling agent. United States Patent US 4650889, 1987.
- [23] Barry, A. Silane Coupling Agents Connecting Across Boundaries v2.0. Gelest Press: Morrisville, 2006.
- [24] Petrie, E. M. Handbook of adhesives and sealants. McGraw Hill: New York, 2000.
- [25] Nanjing capatue chemical Co.,Ltd. Silane Mineral Reaction [Online]. 2007. Available from: <http://www.capatue.com/english/silink/1.asp?maxid=4.html> [2012, January 18]
- [26] Seung, H. C.; Il, D. K.; Jae, M. H.; Ki, H. P.; and Seong, G. O. Effect of the dispersibility of BaTiO<sub>3</sub> nanoparticles in BaTiO<sub>3</sub>/polyimide composites on the dielectric properties. Journal of Materials Letters 61 (2007): 2478 – 2481.

- [27] Hongyan, L.; Gang, L.; Bin, L.; Wei, C.; and Shoutian, C. Dielectric properties of polyimide/ $\text{Al}_2\text{O}_3$  hybrids synthesized by in-situ polymerization. Journal of Materials Letters 61 (2007): 1507 – 1511.
- [28] Tao, H.; Jari, J.; Heli, J.; and Taisto, V. Dielectric properties of BST/polymer composite Journal of the European Ceramic Society 27 (2007): 3997–4001.
- [29] Konno, M.; Kobayashi, Y.; Kosuge, A. The fabrication and dielectric properties of the  $\text{BaTiO}_3$ –polymer nano-composite thin films. Journal of Applied Surface Science 255 (2008): 2723–2729.
- [30] Bhupendra, K. S.; Ajai, K. G.; Dhawan, S. K.; and Gupta, H. C. the preparation and characterization of polyaniline–ZnO composite and its dielectric behavior. Journal of Synthetic Metals 159 (2009): 391–395.
- [31] Wang, F. J.; Li, W.; Xue, M. S.; Yao, J. P.; and Lu, J. S. The preparation of the polyethersulfone (PES)/barium titanate ( $\text{BaTiO}_3$ ) composites. Journal of Composites Part B 42 (2011): 87–91.
- [32] Asliza, A.; Ahmad, Z.; and Ismail, A. B.; Preparation of polyimide/ $\text{Al}_2\text{O}_3$  composite films as improved solid dielectrics. Journal of Materials Science and Engineering 10 (2011): 799-804.
- [33] Kensaku, S.; Jari, J.; Yasuo, M.; and Heli, J. Modification of the dielectric properties of 0–3 ceramic–polymer composites by introducing surface active agents onto the ceramic filler surface. Composite Structures 92 (2010): 1052–1058.
- [34] Chisso corporation chemicals sales department. Calculation of the amount of silane [Online]. 2006. Available from: <http://www.chisso.co.jp/fine/en/ace/calc.html> [2012, January 20]
- [35] Ezhilvalavan, S.; and Tseung, Y. T.; Progress in the developments of  $(\text{Ba,Sr})\text{TiO}_3$  (BST) thin films for Gigabit era DRAMs. Materials Chemistry and Physics 65 (2000): 227–248.

- [36] Jianwen, X.; and Wong, C. P. Characterization and properties of an organic–inorganic dielectric nanocomposite for embedded decoupling capacitor applications. Composites Part A 38 (2007): 13–19.
- [37] Shu, H. X.; Bao, K. Z.; Xiu, Z. W.; Zhi, K. X.; and You, Y. X. Polyimide/BaTiO<sub>3</sub> composites with controllable dielectric properties. Composites Part A 36 (2005): 1152–1157.
- [38] Georgia State University. Polarization of dielectric [Online]. 2000. Available from: <http://hyperphysics.phy-astr.gsu.edu/hbase/electric/dielec.html> [2012, January 22]
- [39] University of Cambridge. The dielectric constant [Online]. 2004. Available from: [http://www.doitpoms.ac.uk/tlplib/dielectrics/dielectric\\_constant.php](http://www.doitpoms.ac.uk/tlplib/dielectrics/dielectric_constant.php) [2012, January 22]
- [40] Giorgos L. The capacitor [Online]. 2009. Available from :[http://pcbheaven.com/wikipages/The\\_Capacitor.html](http://pcbheaven.com/wikipages/The_Capacitor.html) [2012, January 24]

## APPENDICES



## APPENDIX A

### FOURIER TRANSFORM INFRARED SPECTROSCOPY (FTIR) CHARACTERIZATION

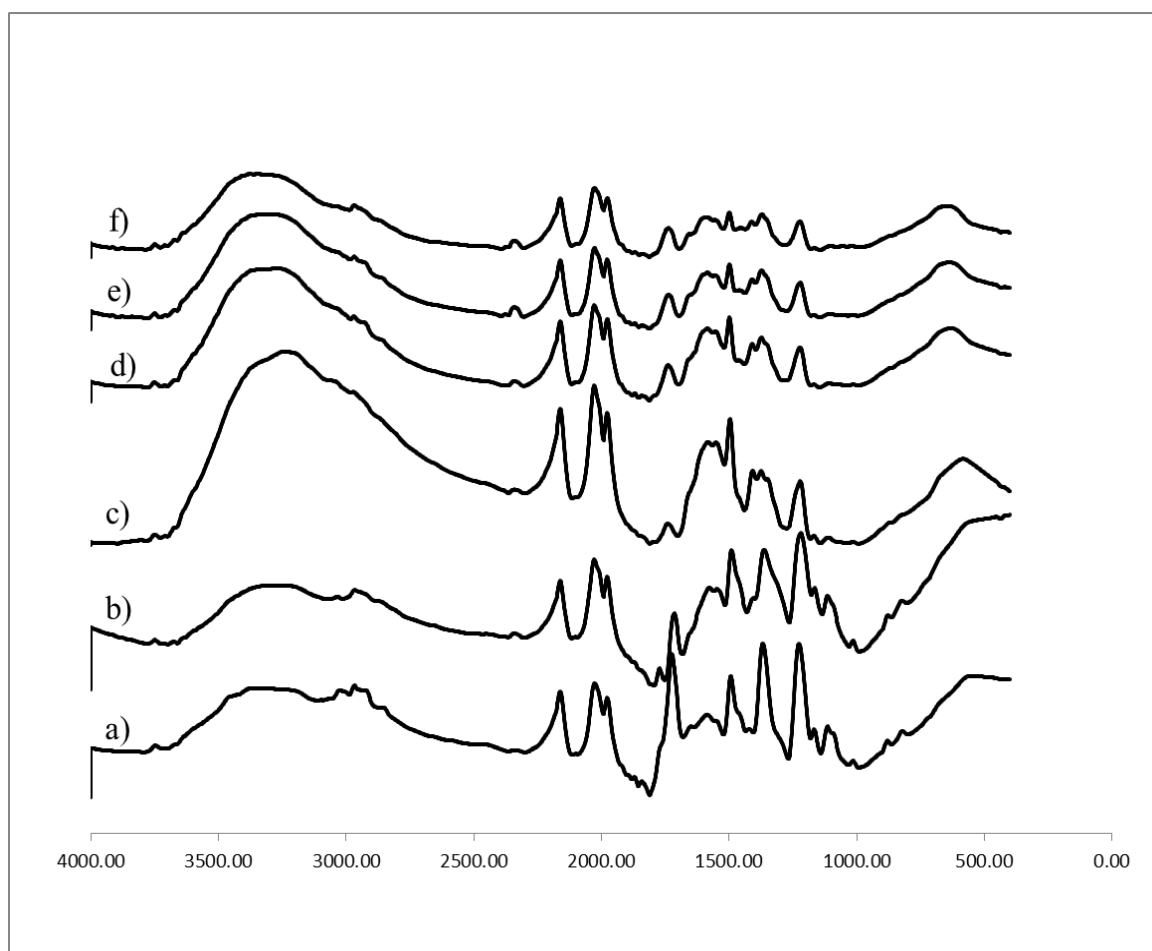


**Figure A.1** FTIR spectra of untreated BST/PI composites a) 70%wt BST b) 80%wt BST c) 90%wt BST d) 93%wt BST e) 95%wt BST f) 97%wt BST

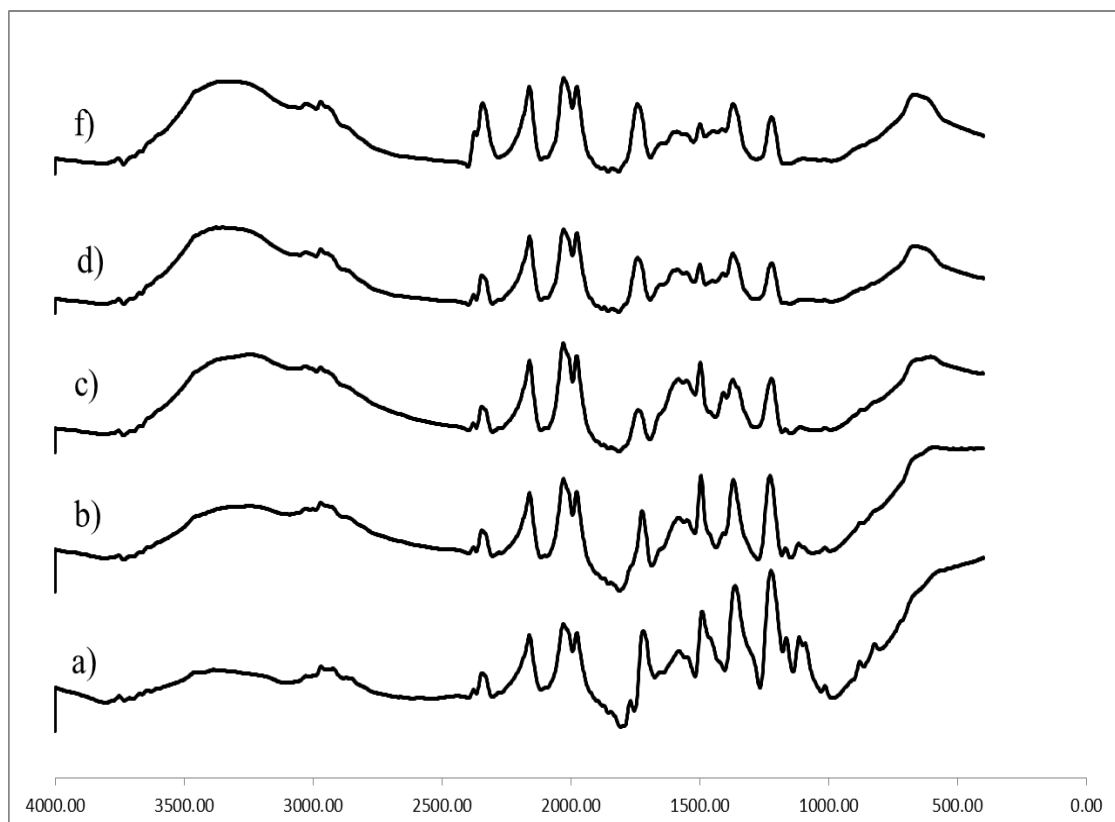


**Figure A.2** FTIR spectra of treated APTS BST/PI composites a) 70%wt BST  
b) 80%wt BST c) 90%wt BST d) 95%wt BST e) 97%wt BST

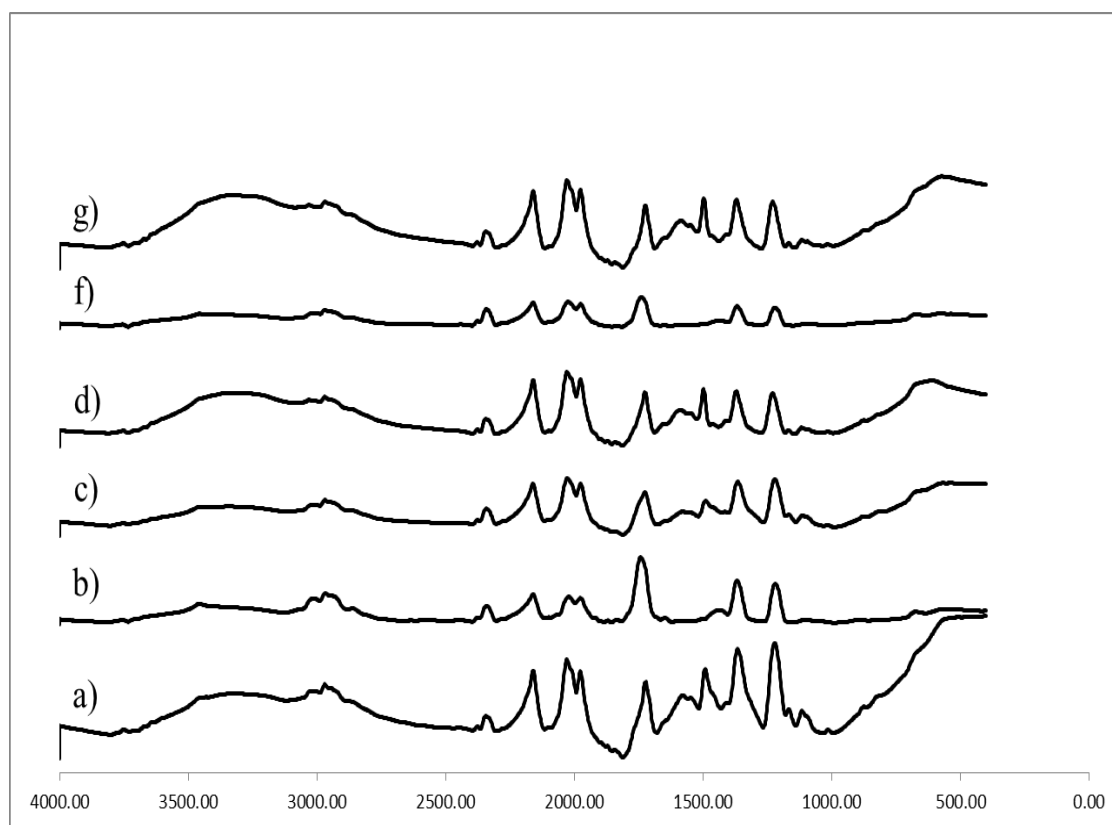


**Figure A.3** FTIR spectra of treated AEAPDS BST/PI composites a) 70%wt BST b) 80%wt BST c) 90%wt BST d) 93%wt BST e) 95%wt BST f) 97%wt BST

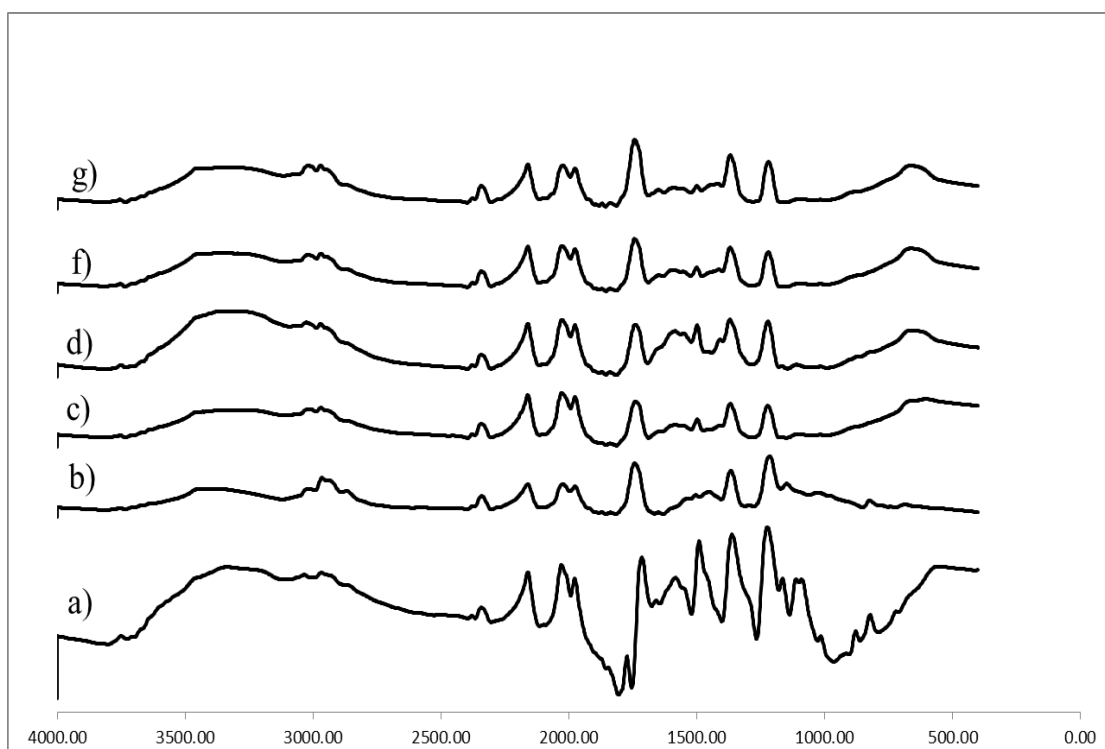


**Figure A.4** FTIR spectra of treated AEEPTS BST/PI composites a) 70%wt BST b) 80%wt BST c) 90%wt BST d) 93%wt BST e) 95%wt BST f) 97%wt BST

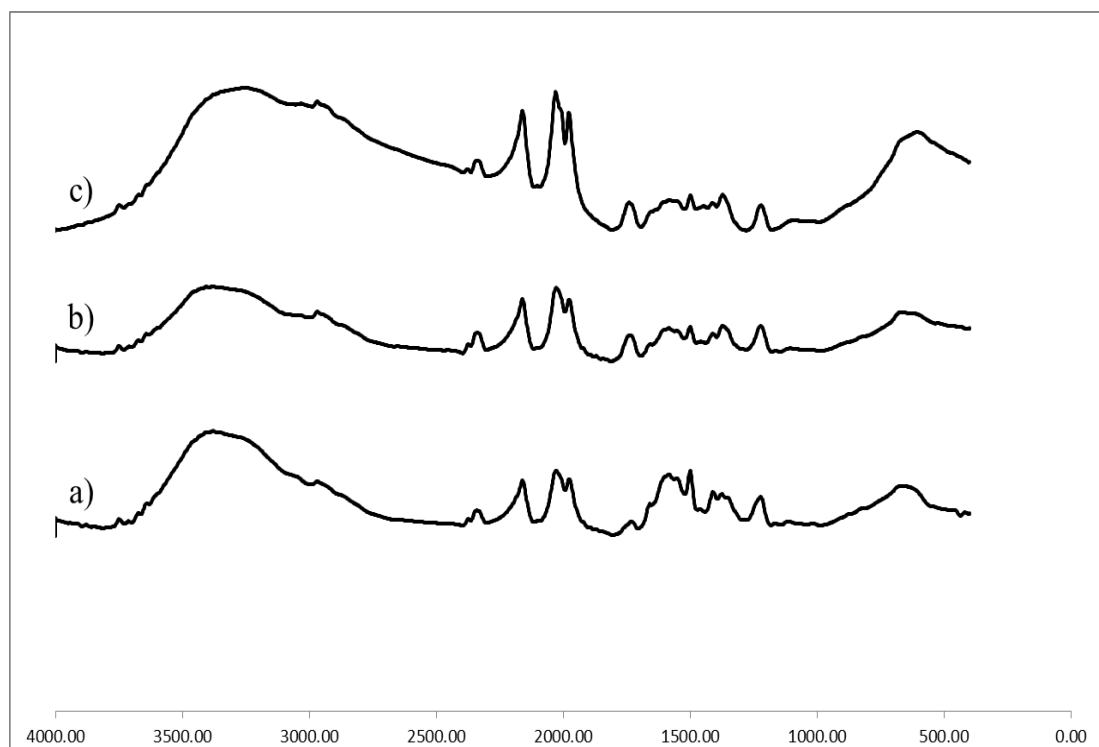


**Figure A.5** FTIR spectra hybrid of treated APTS SrTiO<sub>3</sub>/BST/PI composites  
a) 97%wt (SrTiO<sub>3</sub> 4.85%wt + BST 92.15%wt) b) 97%wt (SrTiO<sub>3</sub> 9.7%wt + BST 87.3%wt) c) 97%wt (SrTiO<sub>3</sub> 24.25%wt + BST 72.75%wt)

## APPENDIX B

### EMBEDDED CAPACITOR

### CHARACTERIZATION

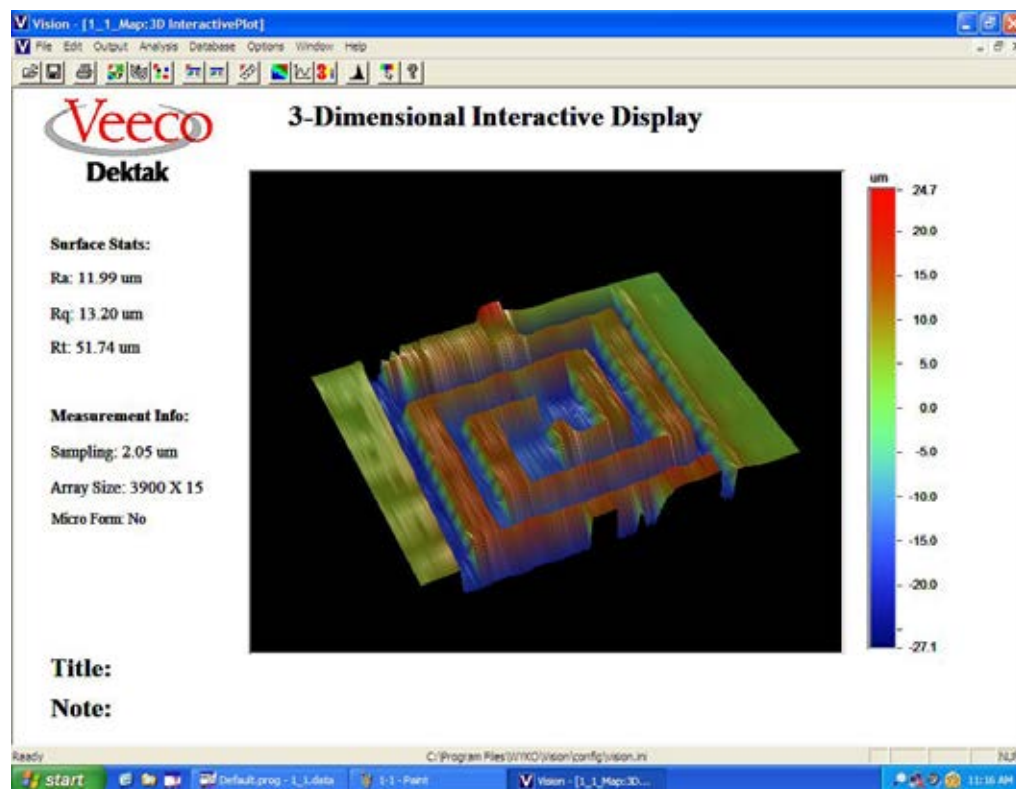


Figure B.1 3D image of embedded capacitor before casting

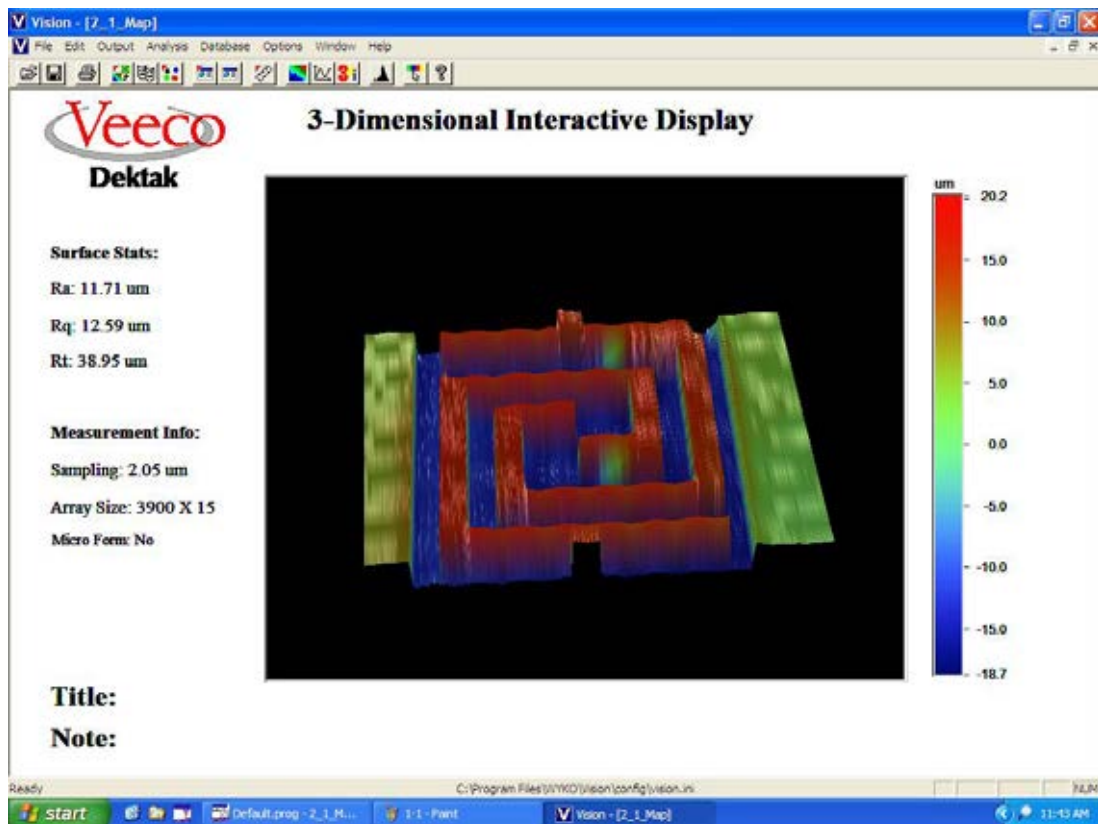
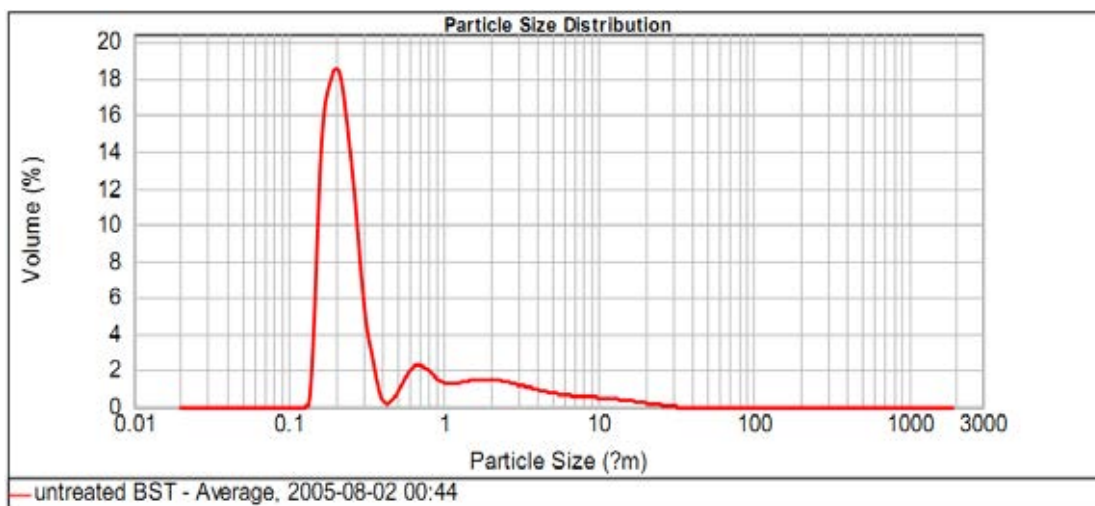


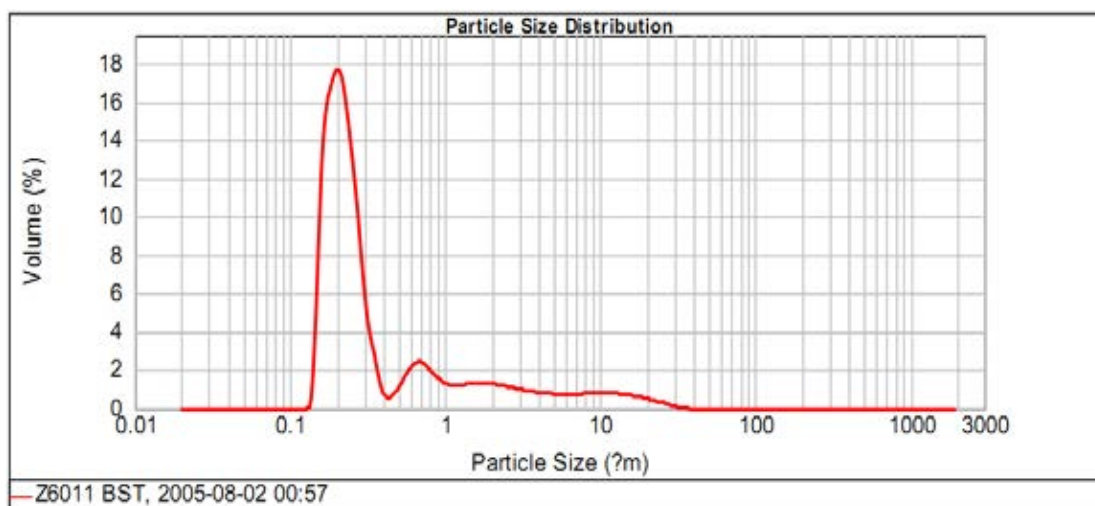
Figure B.2 3D image of embedded capacitor before casting

## APPENDIX C

### THE SIZE DISTRIBUTION OF BST AND SrTiO<sub>3</sub> PARTICLES



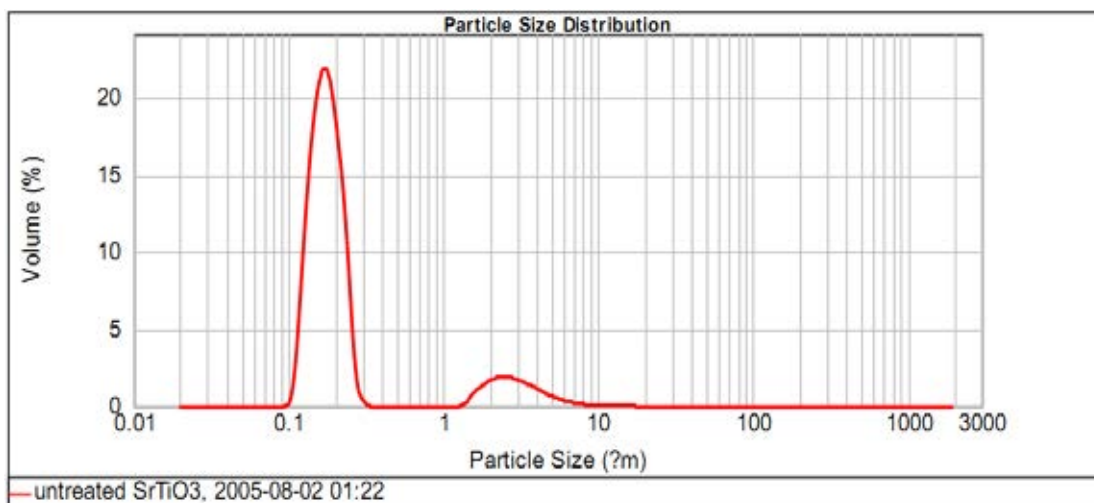
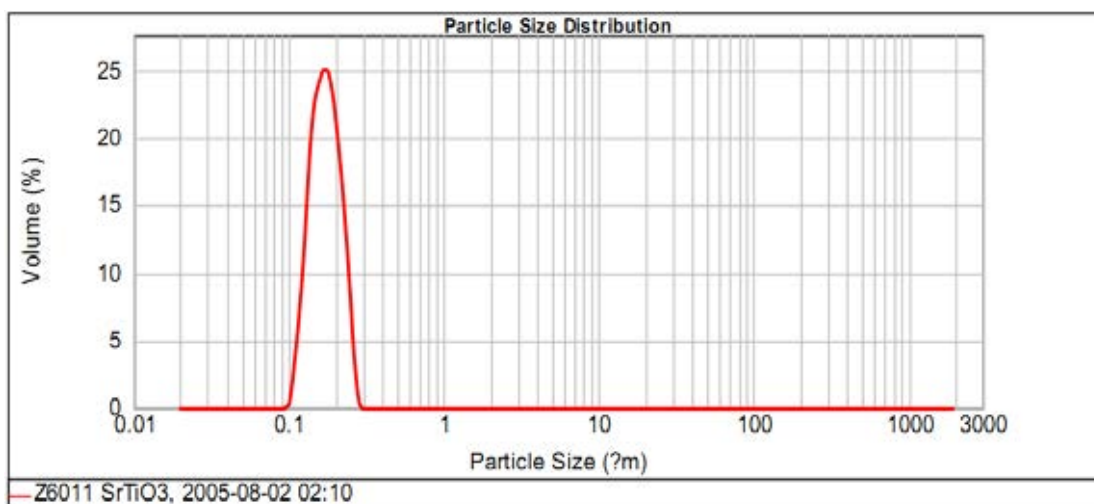
a) Untreated BST



b) APTS silane treated BST

**Figure C.1.** Size distributions of BST particles



a) Untreated SrTiO<sub>3</sub>b) ATPS silane treated SrTiO<sub>3</sub>**Figure C.2.** Size distributions of SrTiO<sub>3</sub> particles

## VITA

Mr. Chawalit Noipara was born on May 1, 1987 in Samutsakhon, Thailand. He received the Bachelor's Degree in Chemical Engineering from Department of Chemical Engineering, Faculty of Engineering, King Mongkut's University of Technology North Bangkok in May 2009, He entered the Master of Engineering in Chemical Engineering at Chulalongkorn University in June, 2010.